ISSN 2523-2517

Volume 5, Issue 14 — January — June — 2021

Journal Electrical Engineering

ECORFAN®

Journal Electrical Engineering, Volume 5, Number 13, January to June, 2021, is a magazine published biannually by ECORFAN-Peru. La Raza Av. 1047 No. - Santa Ana, CuscoPeru. Postcode: 11500. WEB: www.ecorfan.org/republicofperu, revista@ecorfan.org. Editor in Chief: QUINTANILLA - CÓNDOR, Cerapio. PhD. ISSN: 2523-2517. Responsible for the last update of this issue of the ECORFAN Informatics Unit. ESCAMILLA-BOUCHÁN Imelda, LUNA-SOTO, Vladimir, updated June 30, 2021.

Journal Electrical Engineering

Definition of Journal

Scientific Objectives

Support the international scientific community in its written production Science, Technology and Innovation in the Field of Engineering and Technology, in Subdisciplines Electromagnetism, electrical distribution sources, electrical engineering innovation, signal amplification, electric motor design, material science in power plants, management and distribution of electrical energies.

ECORFAN-Mexico, S.C. is a Scientific and Technological Company in contribution to the Human Resource training focused on the continuity in the critical analysis of International Research and is attached to CONACYT-RENIECYT number 1702902, its commitment is to disseminate research and contributions of the International Scientific Community, academic institutions, agencies and entities of the public and private sectors and contribute to the linking of researchers who carry out scientific activities, technological developments and training of specialized human resources with governments, companies and social organizations.

Encourage the interlocution of the International Scientific Community with other Study Centers in Mexico and abroad and promote a wide incorporation of academics, specialists and researchers to the publication in Science Structures of Autonomous Universities - State Public Universities - Federal IES - Polytechnic Universities - Technological Universities - Federal Technological Institutes - Normal Schools - Decentralized Technological Institutes - Intercultural Universities - S & T Councils - CONACYT Research Centers.

Scope, Coverage and Audience

Journal Electrical Engineering is a Research Journal edited by ECORFAN-Mexico S.C in its Holding with repository in Republic of Peru, is a scientific publication arbitrated and indexed with semester periods. It supports a wide range of contents that are evaluated by academic peers by the Double-Blind method, around subjects related to the theory and practice of Electromagnetism, electrical distribution sources, electrical engineering innovation, signal amplification, electric motor design, material science in power plants, management and distribution of electrical energies with diverse approaches and perspectives , That contribute to the diffusion of the development of Science Technology and Innovation that allow the arguments related to the decision making and influence in the formulation of international policies in the Field of Engineering and Technology. The editorial horizon of ECORFAN-Mexico® extends beyond the academy and integrates other segments of research and analysis outside the scope, as long as they meet the requirements of rigorous argumentative and scientific, as well as addressing issues of general and current interest of the International Scientific Society.

Editorial Board

Arbitration Committee

Assignment of Rights

The sending of an Article to Journal Electrical Engineering emanates the commitment of the author not to submit it simultaneously to the consideration of other series publications for it must complement the Originality Format for its Article.

The authors sign the Authorization Format for their Article to be disseminated by means that ECORFAN-Mexico, S.C. In its Holding Republic of Peru considers pertinent for disclosure and diffusion of its Article its Rights of Work.

Declaration of Authorship

Indicate the Name of Author and Coauthors at most in the participation of the Article and indicate in extensive the Institutional Affiliation indicating the Department.

Identify the Name of Author and Coauthors at most with the CVU Scholarship Number-PNPC or SNI-CONACYT- Indicating the Researcher Level and their Google Scholar Profile to verify their Citation Level and H index.

Identify the Name of Author and Coauthors at most in the Science and Technology Profiles widely accepted by the International Scientific Community ORC ID - Researcher ID Thomson - arXiv Author ID - PubMed Author ID - Open ID respectively.

Indicate the contact for correspondence to the Author (Mail and Telephone) and indicate the Researcher who contributes as the first Author of the Article.

Plagiarism Detection

All Articles will be tested by plagiarism software PLAGSCAN if a plagiarism level is detected Positive will not be sent to arbitration and will be rescinded of the reception of the Article notifying the Authors responsible, claiming that academic plagiarism is criminalized in the Penal Code.

Arbitration Process

All Articles will be evaluated by academic peers by the Double-Blind method, the Arbitration Approval is a requirement for the Editorial Board to make a final decision that will be final in all cases. MARVID® is a derivative brand of ECORFAN® specialized in providing the expert evaluators all of them with Doctorate degree and distinction of International Researchers in the respective Councils of Science and Technology the counterpart of CONACYT for the chapters of America-Europe-Asia- Africa and Oceania. The identification of the authorship should only appear on a first removable page, in order to ensure that the Arbitration process is anonymous and covers the following stages: Identification of the Research Journal with its author occupation rate - Identification of Authors and Coauthors - Detection of plagiarism PLAGSCAN - Review of Formats of Authorization and Originality-Allocation to the Editorial Board- Allocation of the pair of Expert Arbitrators-Notification of Arbitration -Declaration of observations to the Author-Verification of Article Modified for Editing-Publication.

Instructions for Scientific, Technological and Innovation Publication

Knowledge Area

The works must be unpublished and refer to topics of Electromagnetism, electrical distribution sources, electrical engineering innovation, signal amplification, electric motor design, material science in power plants, management and distribution of electrical energies and other topics related to Engineering and Technology.

Presentation of the content

As the first article we present, *Analysis of objective functions and weighting parameters syntonization for protection optimization*, by SHIH, Meng Yen, LEZAMA-ZÁRRAGA, Francisco Román, CHAN-GONZALEZ, Jorge de Jesús and SALAZAR-UTIZ, Ricardo Rubén, with affiliation at the Universidad Autónoma de Campeche, as the next article we present, *AC home appliances in a DC home nanogrid*, by CORDOVA-FAJARDO, Miguel Ángel & TUTUTI, Eduardo S., with adscription in the Instituto Tecnológico de Lázaro Cárdenas and Universidad Michoacana de San Nicolás de Hidalgo, respectively, as next article we present, *Prototype simulation for the measurement of energy consumption in watts for alternating current systems*, by HERNÁNDEZ-LUNA, Aldo, CASTRO-JUÁREZ, Ana Magdalena, TORRES-JIMÉNEZ, Jacinto and HERNÁNDEZ-CABRERA, Hugo, from the Instituto Tecnológico Superior de Huauchinango, as last article we present *Analysis of power quality in photovoltaic systems interconnected to the grid*, by DIBENE-ARRIOLA, Luis Martin, FLETES-CAMACHO, Noé Guadalupe, PAREDES-VAZQUEZ, César Paul and MARROQUÍN-DE JESÚS, Ángel, with affiliation at the Universidad Tecnológica de Bahía de Banderas and Universidad Tecnológica de San Juan del Río.

Content

Article	Page
Analysis of objective functions and weighting parameters syntonization for protection optimization SHIH, Meng Yen, LEZAMA-ZÁRRAGA, Francisco Román, CHAN-GONZALEZ, Jorge de Jesús and SALAZAR-UTIZ, Ricardo Rubén *Universidad Autónoma de Campeche*	1-8
AC home appliances in a DC home nanogrid CORDOVA-FAJARDO, Miguel Ángel & TUTUTI, Eduardo S. *Instituto Tecnológico de Lázaro Cárdenas* *Universidad Michoacana de San Nicolás de Hidalgo*	9-13
Prototype simulation for the measurement of energy consumption in watts for alternating current systems HERNÁNDEZ-LUNA, Aldo, CASTRO-JUÁREZ, Ana Magdalena, TORRES-JIMÉNEZ, Jacinto and HERNÁNDEZ-CABRERA, Hugo *Instituto Tecnológico Superior de Huauchinango*	14-19
Analysis of power quality in photovoltaic systems interconnected to the grid DIBENE-ARRIOLA, Luis Martin, FLETES-CAMACHO, Noé Guadalupe, PAREDES-VAZQUEZ, César Paul and MARROQUÍN-DE JESÚS, Ángel *Universidad Tecnológica de Bahía de Banderas* *Universidad Tecnológica de San Juan del Río*	20-31

Analysis of objective functions and weighting parameters syntonization for protection optimization

Análisis de funciones de aptitudes y sintonización de parámetros de pesos para la optimización de protecciones

SHIH, Meng Yen†*, LEZAMA-ZÁRRAGA, Francisco Román, CHAN-GONZALEZ, Jorge de Jesús and SALAZAR-UTIZ, Ricardo Rubén

Universidad Autónoma de Campeche, Campus V, Predio s/n por Av. Humberto Lanz Cardenas y Unidad Habitacional Ecologica Ambiental, Col. Ex-Hacienda Kala, CP 24085, San Francisco de Campeche, Cam., Mexico.

ID 1st Author: *Meng Yen, Shih* / **ORC ID:** 0000-0001-7475-6458, **CVU CONACYT ID:** 408617

ID 1st Co-author: *Francisco Román, Lezama-Zárraga* / **ORC ID:** 0000-0003-3397-7881, **Researcher ID Thomson:** U-1229-2018, **CVU CONACYT ID:** 205493

ID 2nd Co-author: *Jorge de Jesus, Chan-Gonzalez* / **ORC ID:** 0000-0002-8638-1646

ID 3rd Co-author: *Ricardo Rubén, Salazar-Utiz* / **ORC ID:** 0000-0003-2307-737X, **CVU CONACYT ID:** 416277

DOI: 10.35429/JEE.2021.14.5.1.8

Received January 10, 2021; Accepted June 30, 2021

Abstract

The protection coordination problem can be a very complicated task when dealing with meshed networks. Hence, many researchers have formulated the complex coordination problem as an optimization one. Different optimization methods have been proposed for solving the protection coordination problem. However, the different optimization methods are all sensitive to the objective function and the respective weighting parameters. A good optimization method suitable for certain task may not perform successfully if this optimization method does not have the appropriate objective function and/or syntonization of weighting parameters. Therefore, in this article, several proposed objective functions are analyzed and compared. Then the weighting parameters of the proposed objective function are syntonized. Genetic Algorithm is used as a heuristic searching motor for protection optimization. The objective function and the weighting parameters suit different optimization algorithms.

Genetic algorithm, Heuristic optimization, Objective function, Protection optimization, Weighting parameter syntonization

Resumen

El problema de coordinación de protección puede ser una tarea muy complicada cuando se trata de redes mallados. Por tanto, muchos investigadores han formulado el problema complicado de coordinación como un problema de optimización. Diferentes métodos de optimización han sido propuestos para resolver este problema. Sin embargo, todos los diferentes métodos de optimización son sensitivos ante la Función de Aptitud y los Parámetros de Pesos respectivos. Un buen método de optimización adecuado para cierta tarea puede que no ejecute exitosamente si este método no tiene la Función de Aptitud adecuada y/o los Parámetros de Pesos sintonizados. Por lo tanto, en este artículo, varias Funciones de Aptitudes son analizados y comparados. Además, los Parámetros de Pesos de la Función de Aptitud propuesto es sintonizado. El Algoritmo Genético es utilizado como el motor de búsqueda heurístico para la optimización de protección. La Función de Aptitud y los Parámetros de Pesos adapta para los diferentes algoritmos de optimización.

Algoritmo genético, Optimización heurístico, Función de aptitud, Optimización de protección, Sintonización de parámetros de pesos

Citation: SHIH, Meng Yen, LEZAMA-ZÁRRAGA, Francisco Román, CHAN-GONZALEZ, Jorge de Jesús and SALAZAR-UTIZ, Ricardo Rubén. Analysis of objective functions and weighting parameters syntonization for protection optimization. Journal Electrical Engineering. 2021. 5-14:1-8.

*Correspondence to Author (Email: smengyen@uacam.mx)

† Researcher contributing as first author.

Introduction

Protective devices play an important role in the electrical power system for safety, reliability, continuity, voltage quality, service life of primary equipment and life of personnel (Blackburn & Domin 2006). They operate and isolate the electrical network zone under disturbances and/or abnormal operations such as atmospheric discharges, faults caused by animals, accidental short circuits, improper personnel operations etc. (Blackburn & Domin 2006).

Of the different protection devices, the Directional Over Current Relay (DOCR) is widely used in sub-transmission and distribution lines due to its low cost and also offers the virtue of tolerating temporary overloads.

The DOCR has the principle of selective operation. Therefore, in order for the DOCRs to work together properly, they must be coordinated. Coordination states that the relay must provide primary protective operation with the minimum possible time when the fault is located within the protection zone and at the same time provide backup protective operation with a preset time delay when the fault is located in adjacent protection zone (Gers & Holmes 2011, Blackburn & Domin 2006). So, each line or element is protected by at least two protections, or, put another way, having overlapping protection zones.

The coordination of DOCRs is not an exact science, but as an Art it involves some degree of uncertainty due to its complexity, multiple local minima solutions and the use of heuristic optimization methods. So, it is difficult to claim that it has found optimal, but close to optimal, results.

Researchers have devoted their efforts in the study of the DOCR coordination problem, formulating it as an optimization problem and employing different optimization methods to attack this highly complex problem.

Justification

DOCR coordination has evolved from manual, software-assisted, and now heuristic optimization methods.

This evolution can be contributed by some reasons: the nature of the complex DOCRs coordination problem in meshed networks that as the electrical network under study is more meshed and larger, the coordination complexity will be higher (Gers & Holmes 2011); the time delay for performing the complex work manually (Gers & Holmes 2011); and the aspiration for better results that satisfies all DOCRs constraints to establish coordination between protection devices.

Some reported works are: Bedekar & Bhide (2011) proposes coordination of protections using Hybrid Genetic Algorithm (GA); Amraee (2012) proposes implementation of search engine algorithm for optimization of DOCRs; Srivastava, et al (2016) proposes optimization of protections using Particle Swarm (PSO); Saha, et al (2016) proposes computation of protections using teaching-learning based optimization (TLBO).

From the above described, it is aspired to solve the protection coordination problem using optimization methods. However, an appropriate fitness function and the respective suitable weight parameters need to be determined.

Objective

To evaluate the Suitability Functions and tune the weight parameters of the objective subfunctions to suit the GA search engine to solve the DOCRs coordination problem. To analyze and find the conclusion which of the Skill Functions performs better.

Hypothesis

By tuning the weights parameters of the proposed fitness function, it is possible to obtain adequate protection settings results and achieve minimum protection operation times for meshed systems. The proposal perhaps offers better results than the fitness functions proposed in the literatures.

Problem statement

The protections are required to provide primary and backup function with the same set of dial and pickup current settings. So, it is intentionally desired that there be overlapping protection zones.

This is illustrated in Figure 1. It is observed that line $\overline{BC}$ has overlapping protection zones where R1 provides primary operation and R2 provides backup operation for the same line $\overline{BC}$.

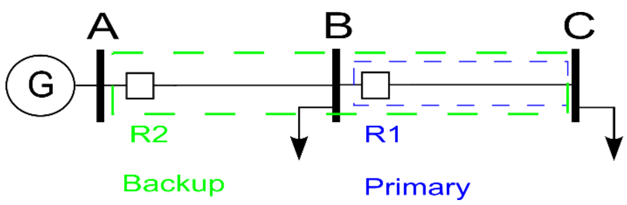

Figure 1 Overlaps of protection zones
Source: Own elaboration

DOCRs have an inverse time characteristic that is defined by the IEEE C37.112-1996 standard. This is presented in equation 1

$$t = \left[\frac{A}{\left(\frac{I_{sc_{max}}}{I_p}\right)^n - 1} + B\right] * dial \quad (1)$$

Where t is the DOCR operation time, $I_{sc_{max}}$ is the maximum fault current, I_p is the inrush current setting, dial is the curve family setting, and A, B, n are IEEE standard constants. In this study, the very inverse characteristic (VI) of IEEE standard is employed which has the values of 19.61, 0.491 and 2 of the constants A, B, n respectively.

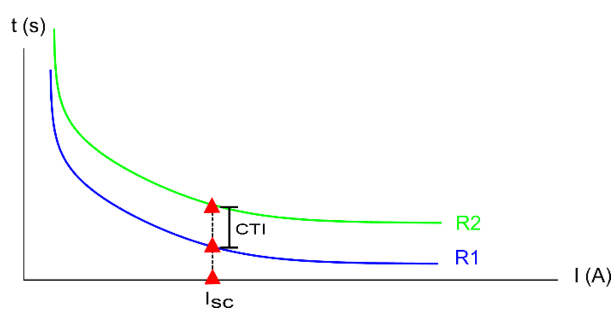

Figure 2 Coordinated primary and backup protection operation of relays R1 and R2
Source: Own elaboration

The operation curves and characteristics of the coordinated relays R1 and R2 are presented in Figure 2. It is observed that they have a coordination time interval (CTI) between them for a given fault current magnitude. In this time-current plane, the horizontal axis represents the current magnitudes in amperes and the vertical axis represents the operating time of the DOCRs in seconds.

Problem suitability functions for optimizing protection settings using genetic algorithm

To optimize the coordination problem and obtain results close to the global optimum, the following conditions must be met: optimization method, a suitable fitness function f(x) and properly tuning the weights of each fitness subfunction.

In this work, we use the GA which is a well recognized algorithm in the computer area for several decades to perform the analysis between the different fitness functions and the proposal. It is also used to tune the weights parameters of the proposed fitness function. The flowchart for the optimization of protections using GA is presented in Figure 3.

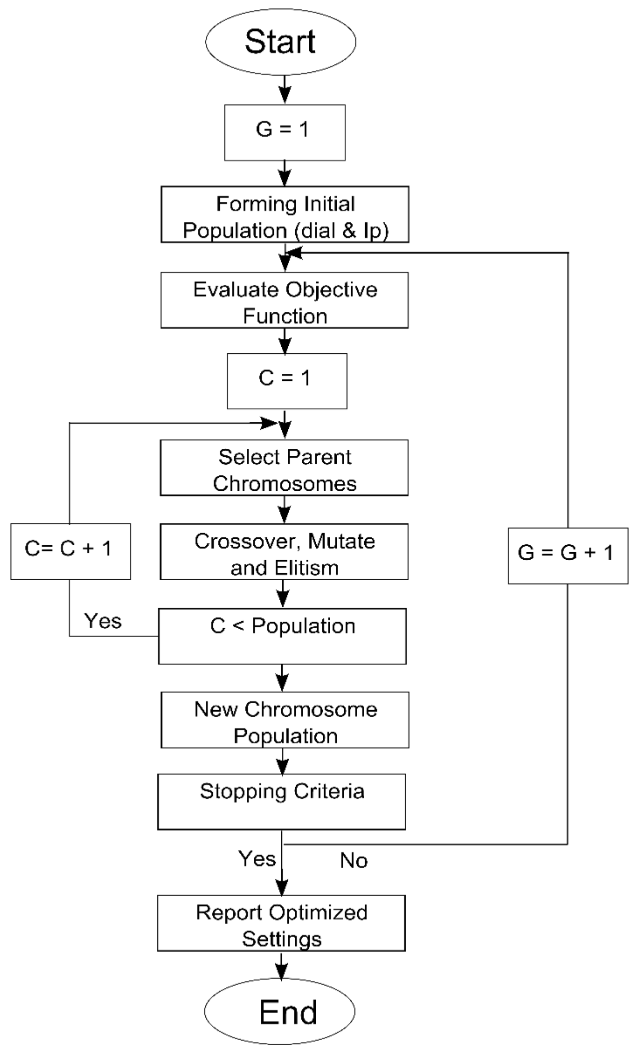

Figure 3 Protection optimization flowchart using GA
Source: Own elaboration

The following table presents the Skills Functions to be studied, both from literatures and the one proposed in this work, in Table 1.

ISSN: 2523-2517

	f(x)	Method	Literatures
I	$\sum_{j=1}^{m} t_{p,j}$	GA, PSO	Zeineldin, et al (2006); Mansour, et al (2007); Bedekar & Bhide (2011); Bedekar & Bhide (2011); Alam, et al (2015).
II	$\sum_{j=1}^{m} t_{p,j} + \sum_{j=1}^{m} t_{b,j}$	TLBO	Saha, et al (2016); Kalage, et al (2016).
III	$\left(\frac{MC}{P}\right) + \alpha\left(\frac{\sum_{j=1}^{P} t_{p,j}}{P}\right) + \beta\left(\frac{\sum_{j=1}^{P} t_{b,j}}{P}\right) + \delta\left(\sum_{L=1}^{P} E_{CTI_L}\right)$	GA	Proposal

Table 1 Skills functions
Source: Own elaboration

The fitness functions of the literatures consist of the summation of primary operation times and backups. While the proposed fitness function has the evaluation of the number of coordination violations, and the Coordination Time Interval (CTI) errors added to the fitness functions in the literatures. Which offers better optimization results.

The parameters: α, β, δ represent the weights affecting each fitness subfunction. MC is the number of coordination losses, P is the number of coordination pairs, t_p is the primary operation time, t_b is the backup operation time, and E_{CTI} is the coordination pair CTI error.

The CTI constraint for selective coordination of protections is expressed mathematically in equation 2:

$$t_b = t_p + CTI \quad (2)$$

The upper and lower bounds of the relay settings in equations 3 and 4 are also presented as optimization constraints:

$$\mathrm{dial}_{\mathrm{min}} \leq \mathrm{dial} \leq \mathrm{dial}_{\mathrm{max}} \quad (3)$$

$$I_{p_{min}} \leq I_p \leq min(I_{sc_{min}}, I_{p_{max}}) \quad (4)$$

Simulation parameters and test systems

In Table 2, the parameters to perform the optimization of protections employing GA and the complexity of the test system are listed. Where the weights parameters δ, τ and ρ will be defined based on the results obtained from weights analysis of the proposed fitness function observing the Pareto Frontier. The number of constraints is the total sum of CTI, $dial$ and I_p.

Parameters	Values
CTI	0.3
dial	[0.05:2.0]
Ip	[1.4:1.6]*Icarga
α, β, δ	To be defined, Pareto Frontiers analysis
Population	100
Generations	2,000
No. of lines	5
No. of DOCRs	10
No. of decision variables	20
No. of restrictions	36

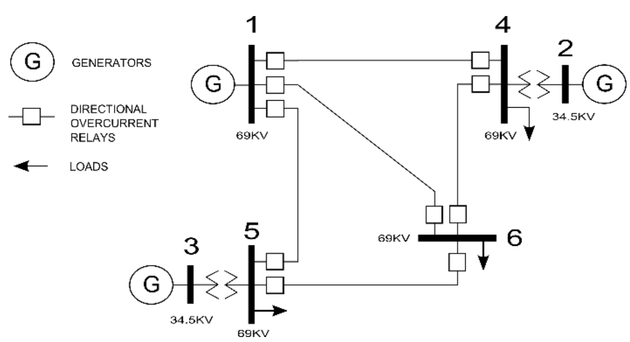

Figure 4 The 6-bus meshed test system
Source: Hadi Saadat, Power system analysis, McGraw-Hill, ISBN 0-07-561634-3, 1999

Table 3 shows the line parameters. Where R is the resistance, X is the reactance and 1/2B is the shunt admittance.

Bus	Bus	R	X	1/2 B
1	4	0.035	0.225	0.0065
1	5	0.025	0.105	0.0045
1	6	0.040	0.215	0.0055
2	4	0.000	0.035	0.0000
3	5	0.000	0.042	0.0000
4	6	0.028	0.125	0.0035
5	6	0.026	0.175	0.0300

Table 3 Line parameters
Source: Hadi Saadat, Power system analysis, McGraw-Hill, ISBN 0-07-561634-3, 1999.

Table 4 shows the parameters of transient reactance, voltage, active and reactive powers of generations and loads.

ISSN: 2523-2517

Bus	X'd	Generation V	MW	Limites Mvar Min	Max	Charge MW	Mvar
1	0.20	1.060					
2	0.15	1.040	50	0	40		
3	0.25	1.030	30	0	20		
4						100	70
5						30	5
6						20	5

Table 4 Slightly modified generator and load parameters
Source: Hadi Saadat, Power system analysis, McGraw-Hill, ISBN 0-07-561634-3, 1999

The IEEE 14-bus system will be used for the analysis and tuning of proposed fitness function weights and the topology is presented in Figure 5. The system is an approximation of American Electric Power System in February 1962 consisting of 14 buses, 5 generators and 11 loads.

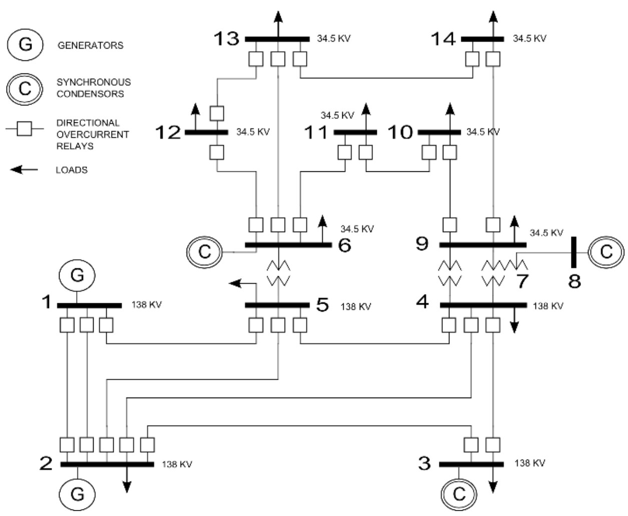

Figure 5 The IEEE 14 bus test system
Source:http://labs.ece.uw.edu/pstca/pf14/pg_tca14bus.htm

The line parameters, as well as the transient reactance's of generators, voltages, active and reactive powers of generations and loads are standardized data and can be found at (http://labs.ece.uw.edu/pstca/pf14/pg_tca14bus.htm).

It is worth mentioning that slight modifications were made for both systems in order to adapt the transmission system to the sub-transmission voltage level where the relay protection principle under study is implemented.

Simulations and results

In Table 5, the tuning results of the weights (α, β and δ) of the proposed fitness function are presented.

The weights parameters α, β and δ are evaluated between the interval [0.25:0.25:2]. Therefore, it has a total of 512 combinations. Each combination was evaluated in 50 simulations of the IEEE 14-bus system meshed over 2,000 generations. Subsequently, the average fitness function, the number of coordination losses and their respective standard deviations, as well as the averaged primary operation times, backups and CTIs are presented in Table 5, but to save space, only the best tuning combinations are presented, from which plot the Pareto Frontier plots presented in Figures 6, 7 and 8.

It can be observed from Figure 6, that the minimum primary operation time occurs when the weight parameter α increases up to 2. Which reveals that the best tuning for the weight parameter α is 2.

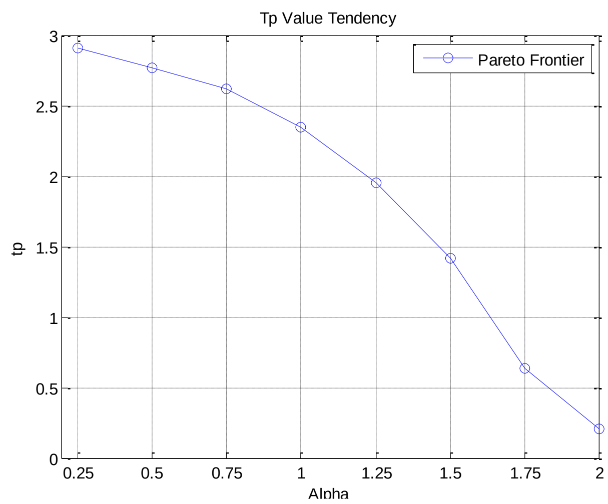

Figure 6 Pareto frontier of the weight parameter α and the trend of primary operation time
Source: Own elaboration

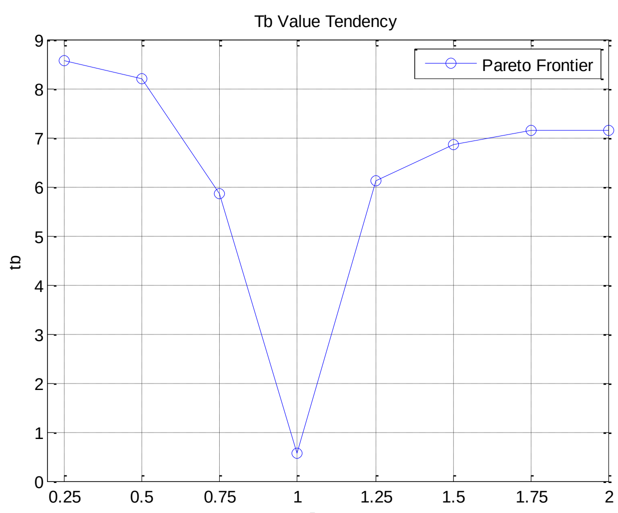

Figure 7 Pareto frontier of the weight parameter β and the trend of the operating time backup
Source: Own elaboration

ISSN: 2523-2517

It can be observed from Figure 7, that the minimum backup operation time occurs when the weight parameter β is located at the value 1. Which reveals that the best tuning for the weight parameter β is 1.

	α	β	δ	f(x)	f(x)-SD	MC	MC-SD	tp	tb	CTI
tp	**0.25**	1	2	8.71	0.72	0.00	0.00	**2.91**	7.90	5.00
	0.5	1	2	9.04	0.62	0.00	0.00	**2.77**	7.58	4.81
	0.75	1	2	9.39	0.66	0.00	0.00	**2.62**	7.34	4.73
	1	1	2	9.05	0.76	0.00	0.00	**2.35**	6.63	4.28
	1.25	1	2	8.08	0.66	0.00	0.00	**1.95**	5.57	3.61
	1.5	1	2	6.22	0.69	0.00	0.00	**1.41**	4.02	2.61
	1.75	1	2	2.96	0.45	0.00	0.00	**0.64**	1.78	1.15
	2	1	2	0.98	0.01	0.00	0.00	**0.21**	0.56	0.36
tb	2	**0.25**	2	7.06	0.56	0.00	0.00	2.42	**8.56**	6.14
	2	**0.5**	2	9.22	0.79	0.00	0.00	2.52	**8.20**	5.68
	2	**0.75**	2	8.34	0.61	0.00	0.00	1.94	**5.86**	3.92
	2	**1**	2	0.98	0.01	0.00	0.00	0.21	**0.56**	0.36
	2	**1.25**	2	12.08	1.00	0.00	0.00	2.18	**6.12**	3.94
	2	**1.5**	2	15.16	1.29	0.00	0.00	2.40	**6.85**	4.45
	2	**1.75**	2	17.85	1.28	0.00	0.00	2.63	**7.16**	4.53
	2	**2**	2	19.67	1.74	0.00	0.00	2.65	**7.14**	4.49
CTI	2	1	**0.25**	11.89	6.73	0.00	0.00	2.34	7.21	**4.87**
	2	1	**0.5**	3.48	0.72	0.00	0.00	0.74	1.99	**1.25**
	2	1	**0.75**	2.18	0.28	0.00	0.00	0.46	1.25	**0.79**
	2	1	**1**	1.48	0.27	0.00	0.00	0.31	0.85	**0.54**
	2	1	**1.25**	1.25	0.16	0.00	0.00	0.26	0.72	**0.46**
	2	1	**1.5**	1.10	0.14	0.00	0.00	0.23	0.63	**0.41**
	2	1	**1.75**	1.02	0.04	0.00	0.00	0.21	0.59	**0.38**
	2	1	**2**	0.98	0.01	0.00	0.00	0.21	0.56	**0.36**

Table 5 Parameter tuning of weights α, β and δ, for optimization
Source: Own elaboration

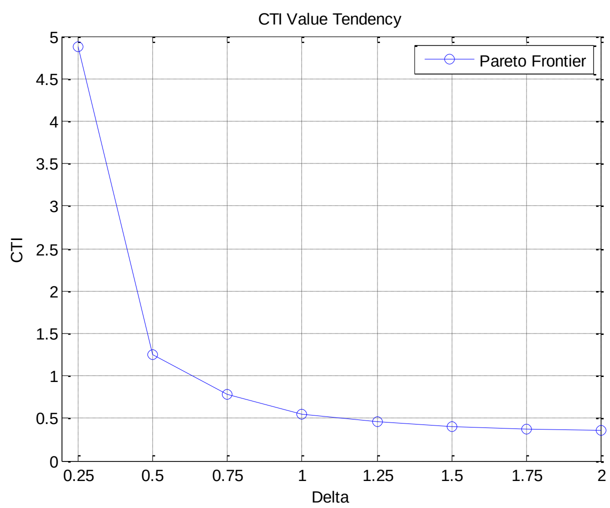

Figure 8 Pareto frontier of the weight parameter δ and the trend of the operating time CTI
Source: Own elaboration

It can be observed from Figure 8, that the minimum CTI operation time occurs when the weight parameter δ is located at the value 2. Which reveals that the best tuning for the weight parameter δ is 2.

Therefore, from Figures 6, 7 and 8 it can be observed that the best values for the weight parameters α, β and δ of the proposed fitness function is 2, 1, 2 when it obtains minimum results, since it is a DOCRs time minimization problem. Which were plotted from the data in Table 5, where it can be concluded that the weights 2, 1, 2 give better results and are shaded in golden color.

The plotted values from Table 5 for each weight parameter are in bold and color.

Next, the results of comparison of skill functions I, II, and III are presented in Table 6. The average values and standard deviation of DOCRs operation times in 50 independent simulations are analyzed.

		GA			
		tp(seg)	tb(seg)	CTI(seg)	MC
I	**Average**	0.34	0.90	0.56	16
	SD	0.01	0.03	0.03	--
II	**Average**	0.34	0.88	0.54	14
	SD	0.01	0.02	0.02	--
III	**Average**	0.46	1.13	0.67	0
	SD	0.02	0.07	0.05	--

Table 6 Average results and standard deviation of DOCRs operation times and coordination losses in 50 runs of independent simulations of skill functions I, II and III
Source: Own elaboration

It is observed from Table 6 that for the three skill functions, in spite of starting with random populations, all the simulations manage to converge, since they have a standard deviation (SD) of the operation times in the order of thousandths. In addition, it is observed that the times of primary operations, backup and CTI are in a very acceptable range of operation of protections. However, the key differentiating factor that highlights the superiority of the proposed fitness function (III) is that it has zero coordination loss. While the fitness functions I and II have 16 and 14 runs with coordination losses respectively. Which means that some line(s) are not adequately protected. And there may be cases of simultaneous firing or that the backup comes into function before the primary. From here the great advantage of the proposed suitability function (III) is revealed that all lines are protected by the protections adequately.

It is worth mentioning that the values of the three suitability functions were not compared because as they are different suitability functions they result in a different value. Therefore, they cannot be compared.

In Table 7, the result of a simulation run with the proposed fitness function (III) is presented. It can be observed that the primary times, backups, CTI, are very practical. The primary and backup fault currents, protection coordination couples are also presented.

Primary	Backup	GA			Primary	Backup
		tp(s)	tb(s)	CTI(s)	Icc(A)	Icc(A)
4 6	1 4	0.44	1.15	0.71	7493	2338
1 5	4 1	0.64	2.23	1.60	7676	1900
1 6	4 1	0.37	2.19	1.81	8572	1921
5 6	1 5	0.43	0.75	0.31	6554	3676
1 4	5 1	0.33	0.77	0.43	7955	2363
1 6	5 1	0.37	0.73	0.36	8572	2508
6 4	1 6	0.48	0.93	0.45	4370	2127
6 5	1 6	0.48	0.88	0.40	5366	2231
1 4	6 1	0.33	1.33	1.00	7955	1451
1 5	6 1	0.64	1.09	0.45	7676	1633
6 1	4 6	0.32	0.89	0.56	5620	3186
6 5	4 6	0.48	0.92	0.44	5366	3104
4 1	6 4	0.44	0.97	0.53	7590	2433
6 1	5 6	0.32	0.87	0.55	5620	2405
6 4	5 6	0.48	0.96	0.48	4370	2216
5 1	6 5	0.54	0.86	0.32	5291	2413
AVERAGE		0.44	1.09	0.65	--	--

Table 7 Primary, backup, CTI and fault currents of the coordination pairs of a simulation run
Source: Own elaboration

It can be emphasized that the CTI times meet the constraint presented in equation 2, this reveals that all protection couples are coordinated and there is no coordination loss. The average primary, backup and CTI times of the 6-bus meshed system in a simulation run are: 0.44, 1.09, 0.65 seconds respectively.

The optimized DOCRs settings of the same simulation run are presented in Table 8. Using the proposed fitness function (III) it can be observed that it channels the algorithm towards minimizing the times of primary operations, backups and CTI using small dial parameters and overload factor for the starting current. Thus, this allows the protections to operate faster in the event of electrical faults in the lines.

DOCR	GA	
	dial	Ip
1 4	0.53	654
4 1	0.67	675
1 5	1.23	286
5 1	0.99	283
1 6	0.69	436
6 1	0.52	448
4 6	0.70	621
6 4	0.56	595
5 6	0.75	437
6 5	0.78	418

Table 8 Dial and inrush current settings for the overcurrent relays of a simulation run
Source: Own elaboration

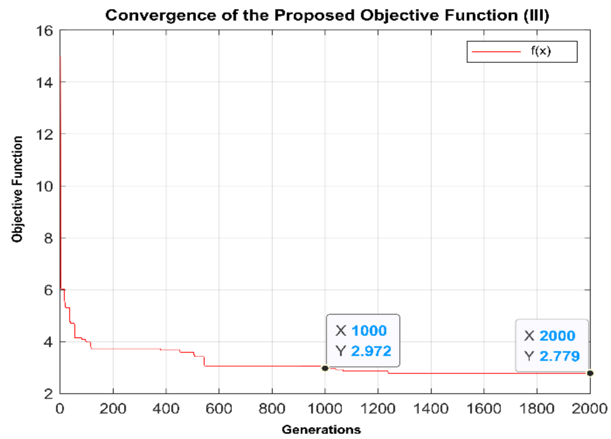

Figure 9 Convergence of the GA for the 6-bus system meshed from a simulation run
Source: Own elaboration

Figure 9 presents the GA convergence trend using the proposed fitness function (III) for the optimization of protections in a simulation run. It is observed that the fitness function is decreasing, which reveals that the proposed fitness function is guiding the algorithm towards the search for minimum results of operation times.

On the other hand, it can be detected that there are only slight improvements to the results after 1,000 generations. It has as 2,972 in the 1,000th generation and 2,799 in the 2,000th generation. In other words, it reveals that the coordination problem has been solved since at 1,000 generations it has almost converged to the proposed fitness function (III). Therefore, the running time of the algorithm for optimization could have been halved if desired by the user by setting the convergence criterion as 1,000 generations. It is worth mentioning that the GA algorithm with the proposed fitness function (III) requires approximately and only 130 seconds to run and evaluate the two thousand generations for the coordination of DOCRs.

Acknowledgement

The authors are grateful for the support and effort of the Universidad Autónoma de Campeche for its researchers to disseminate the research topics in which they are immersed.

Conclusions

The coordination of protections manually is a very complex work that can take a long time. However, caution should be exercised when opting for the support of optimization algorithms to solve this problem.

As shown in the study results in this article, the algorithms converge to different results (settings) when different skill functions are used. Some of them lead to the loss of coordination of protections, leaving some line(s) without protection in case of power failure scenarios.

Therefore, a proper suitability function proposal for this problem is of utmost importance. In addition, proper tuning of the weights of the fitness function is crucial. Since, without proper weights, the algorithm may get lost in the multiple local minima and giving results as coordination losses as well.

It is concluded from the studies conducted that the objective has been met and the hypothesis is affirmative. The proposed fitness function (III) is adequate and the study of tuning weights are appropriate for electrical networks with diverse connectivity and complexity.

References

Alam M.N., Das B. and Pant V. (November 2015). A comparative study of metaheuristic optimization approaches for directional overcurrent relays coordination, *Electric Power Systems Research*, 128, 39-52.

Amraee T. (July 2012). Coordination of Directional Overcurrent Relays Using Seeker Algorithm. *IEEE Transactions on Power Delivery*, 27 (3), 1415-1422.

Bedekar P. & Bhide S. (January 2011). Optimum coordination of directional overcurrent relays using the hybrid GA-NLP approach. *IEEE Transactions on Power Delivery*, 26 (1), 109-119.

Bedekar P. & Bhide S. (September 2011). Optimum coordination of overcurrent relay timing using continuous genetic algorithm. *Elsevier Expert Systems with Applications*, 38 (9), 11286-11292.

Blackburn J. L. & Domin T. J. (2006). *Protective relaying, principles and applications*. (3rd edition). CRC Press Taylor & Francis Group.

Gers J. M. & Holmes E. J. (2011). *Protection of Electricity Distribution Networks*. (3rd edition). IET.

IEEE Standard Inverse-Time Characteristic Equations for Overcurrent Relays, IEEE std C37.112-1996.

Kalage A.A. and Ghawghawe N.D.. (March 2016). Optimum coordination of directional overcurrent relays using modified adaptive teaching learning based optimization algorithm, *Springer Intelligent Industrial Systems*., 2 (1), 55-71.

Mansour M.M., Mekhamer S.F., and El-Kharbawe N.E-S.. (July 2007). A modified particle swarm optimizer for the coordination of directional overcurrent relays, *IEEE Transactions on Power Delivery*, 22 (3), 1400-1410.

Othman A.M. and Abdelaziz A.Y.. (2016). Enhanced Backtracking Search Algorithm for Optimal Coordination of Directional Over-current Relays Including Distributed Generation, *Electric Power Components and Systems*, 44 (3), 278-290.

Saadat H. (1999). *Power system analysis*. McGraw-Hill.

Saha D., Datta A., Saha B.K. and Das P.. (March 2016). A comparative study on the computation of directional overcurrent relay coordination in power systems using PSO and TLBO based optimization, *Engineering Computations*., 33 (2), 603-621.

Srivastava A., Tripathi J.M., Mohanty S.R. and Panda B.. (2016). Optimal Over-current Relay Coordination with Distributed Generation Using Hybrid Particle Swarm Optimization–Gravitational Search Algorithm, *Electric Power Components and Systems*, 44 (5), 506-517.

Zeineldin H., El-Saadany E. & Salama M. (July 2006). Optimal coordination of overcurrent relays using a modified particle swarm optimization. *Electric Power Systems Research*, 76 (11), 988-995.

Article

Journal Electrical Engineering

June 2021, Vol.5 No.14 9-13

AC home appliances in a DC home nanogrid

Electrodomésticos de CA en una nanored doméstica de CD

CORDOVA-FAJARDO, Miguel Ángel*† & TUTUTI, Eduardo S.

Instituto Tecnológico de Lázaro Cárdenas, Tecnológico Nacional. Department of Basic Sciences. Lazaro Cardenas, Michoacan. México.

Universidad Michoacana de San Nicolás de Hidalgo, School of Physical and Mathematical Sciences. Morelia, Michoacán. México.

ID 1st Author: *Miguel Ángel, Cordova-Fajardo* / **ORC ID:** 0000-0001-9844-1979, **CVU CONACYT ID:** 490783

ID 1st Co-author: *Eduardo S., Tututi* / **ORC ID:** 0000-0002-0126-6615, **CVU CONACYT ID:** 13704

DOI: 10.35429/JEE.2021.14.5.9.13

Received January 15, 2021; Accepted June 30, 2021

Abstract

In order to satisfy needs at home, a way of incorporating renewable energy sources, storage devices and home appliances into a Direct Current Home Nanogrid, is shown. This technological option could increase the participation of the end users in the energy market. Currently, the electric system transition from Altern Current to Direct Current systems is easier due the availability of cheapest DC home appliances. Finally, we demonstrate that the energy saving when the DC home nanogridis used, it represents around of 15 %.

Energy democracy, Direct current, Efficiency

Resumen

Se muestra una manera de incorporar dentro de una Nanored Doméstica de Corriente Directa, fuentes de energía renovable, sistemas de almacenamiento de energía, así como electrodomésticos con el objetivo de satisfacer las necesidades de un hogar. La propuesta tecnológica pretende incrementar la participación del usuario final en la toma de decisiones dentro del mercado energético. La transición de un sistema eléctrico en base a Corriente Alterna hacia un sistema de Corriente Directa se facilita con la existencia de electrodomésticos de CD en el mercado local. Finalmente, se muestra una reducción en el consumo de energía alrededor del 15% con el uso de Corriente Directa.

Democracia energética, Corriente directa, Eficiencia

Citation: CORDOVA-FAJARDO, Miguel Ángel & TUTUTI, Eduardo S. AC home appliances in a DC home nanogrid. Journal Electrical Engineering. 2021. 5-14:9-13.

* Correspondence to Author (Email: mangel.cordova@lcardenas.tecnm.mx, eduardo.tututi@umich.mx)

† Researcher contributing as first author.

Introduction

The incorporation of renewable energy sources (RES) into electric systems has promoted the emergence of distributed systems. This is a commitment in sustainable systems, with the aim of considerably reduce the emission of greenhouse gases in the electrical energy generation process. The fundamental concept for the development of distributed systems has been mainly focused on microgrids. A microgrid is performed by different sectors. Firstly, the energy generation sector, with a strong tendency to incorporate RES (wind and photovoltaic power plants). The next is the distribution sector that is composed of the wiring that feeds the load sector. In order to ensure the reliability and stability of the microgrid, the energy management sector (EMS) is able to provide information about generation and consumption of the energy. The advantage of the distributed systems lies in avoid the energy loss due the transmission of energy over long distances as well as the ease of integrating RES, which generate energy close to the end users. However, distributed systems operate with a similar dynamic to the traditional centralized systems, for which the flow of energy originates from large renewable energy parks or power plants to end users. On the other hand, RES has promoted the development of awareness in members of the society who are concerned about phenomena such as global warming or climate change.

Currently, it is sought to achieve increasingly efficient electrical systems, for which it has been incurred in the development of systems based on Direct Current (DC). These kinds of systems have proven to be greater energy efficiency, with lower losses and better performance in a simple and an easier way with respect to systems based on Alternating Current (AC). The growth of DC systems has been limited due to a wide dominance of AC systems in the energy market, to the extent that there is a lack of DC appliances (Moussa, Jebali-Ben Ghorbal, & Slama-Belkhodja, 2018). This is a critical factor for the migration to DC systems by the end user.

It is intended that the DC home nanogrids (DCHN's) are established as a technological development, involving renewable energy sources and energy storage systems, which in turn provides greater opportunity for end user participation in the energy market.

With the technological changes driven by RES and new energy storage system (ESS), it is intended to develop an electrical system aimed at the domestic sector, which incorporates RES and ESS to meet needs and diminish dependence on the public grid. In principle, the characteristics that such a system must meet is to be simple and easy, attractive and viable for the end user from the economic and efficiency aspects.

This paper presents the technological development of a DCHN, oriented to satisfy the daily needs of a house with the incorporation of RES and ESS. It shows the possibility of using high efficiency household appliances initially designed to operate in AC, working inside a DCNH with slight, or without, modifications.

This article is structured as follows: in the *General configuration of nanogrid, an* overview of the sectors that make up the nanogrid is described. In the *Voltage level* section, various reported voltage levels are shown. The *DCHN Configuration section* describes the nanogrid developed in this research. The *Appliance Selection section* establishes criteria and it mentions the appliances used. The section *Appliance behavior within the DCHN* presents experimental readings. It continues with the *Results* section followed by *Acknowledgments* and finally the *Conclusions* section.

General configuration of the nanogrid

Recently, the design of electrical systems has focused on their optimization, with the aim of achieving more efficient systems. In order to reduce energy losses, high efficiency appliances are incorporated, whose power electronics employed, gives them a non-linear behavior. The nature of these loads represents a great challenge for the stability of electrical systems.

Within the nanogrid, like the microgrids, sectors with specific functions are identified. The first sector that we will describe is the energy generation sector. In this sector is carried out the generation of energy with a predisposition towards renewable energy sources. Nowadays, the energy storage sector has taken great importance, mainly due to the impulse in the development and commercialization of electric cars.

This has allowed a drastic reduction in price, weight and size of batteries. Therefore, the integration of energy storage devices within a DCHN is feasible.

The distribution sector consists of the wiring through which energy is transmitted to the load sector. In the power transmission processes such as the Joule effect become very relevant for the sizing and design of the wiring. Regarding the load sector, this is characterized by the presence of high efficiency appliances with a non-linear behavior. The electrical protection system will be occup of limiting damages and avoiding the propagation of undesired phenomena such as short circuit or overload within the system. In a condition of a gradual discharge inside the storage sector that compromises the stability of the system and/or the useful life of the batteries, it can be taken as a function of the protection systems, it is to emphasize that this condition corresponds to a function of the EMS. In this sector, the data collection of the energy generation and consumption process is carried out; the parameters for an optimal operation of the system are established. For this sector is visualized a wide area of study to be carried out for future research linked to the concept of "Smart Home".

Voltage level

Among the typical applications of DC electrical systems can be mentioned mainly the automotive sector. In which the voltage level range between 12 and 24 VDC, being able to reach values of 48 VDC. In industrial applications, the usual voltages are considered high voltage levels such as 380 VDC. Historically, we back to the firsts electrical systems developed by Thomas Edison which used DC (AILee & Tschudi, 2012). The voltage level used in those systems corresponded to a value of 100 VDC (Barazarte, 2013). The selection of the operating voltage level in the DCHN is a critical step. Currently, DC nanogrids with different voltage levels have been proposed, many of them based on automotive applications involving low voltages equivalent to 12VDC.

These incorporate appliances designed for those voltage levels. In addition, the configurations of a DC nanogrid have been diversified, coming to establish buses with different voltage levels according to the appliances, with a voltage range from 12, 24, 48, 380 VDC. Each of these buses is interconnected between them by means of converters whose function is to stabilize the voltage level in the buses.

DCHN Configuration

The proposed configuration in this research is shown in Fig. 1. The energy generation sector of the DCHN is performed by 5 photovoltaic panels with a power of 250 watts each. Our energy storage sector is made up by a battery set of 10 batteries, it should be noted that this battery set is taken from an electric vehicle. The nominal voltage of each battery corresponds to 12 VDC, which establishes a nominal voltage for the battery set of 120 VDC, as well as for the distribution and load sectors (Cordova-Fajardo & Tututi Hernández, 2019). Each photovoltaic panel has the capacity to supply power to a pair of batteries with a voltage of 24 VDC. The distribution sector is formed by a distribution bus, for which, it is used the same wiring intended for AC systems. This makes easy to implement a DCHN in a typical AC home. This includes the contacts, switches, plugs and other accessories.

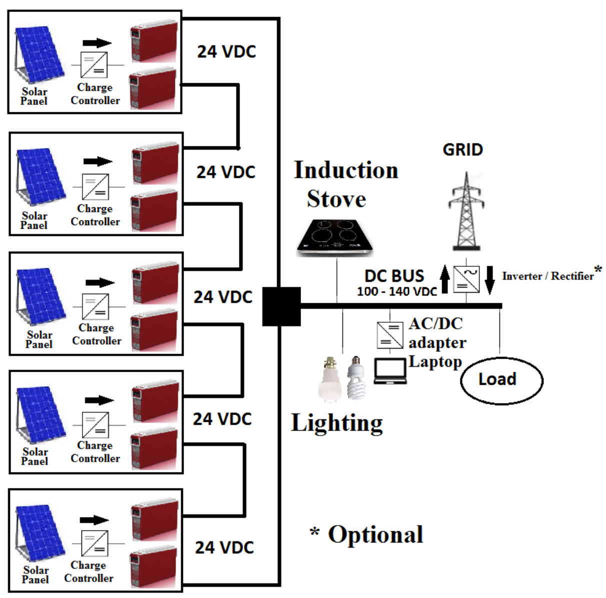

Figure 1 Proposed configuration for CDHN
Source: (Cordova-Fajardo & Tututi Hernández, 2019)

ISSN-2523-2517

June 2021, Vol.5 No.14 9-13

Selection of Appliances

In this section, we focus on the search and selection of appliances available in the local market to incorporate them into the DCHN. The process of converting electrical energy into useful work, in other words, the consumption of energy to meet our daily needs within the home, is carried out by the appliances located in our load sector. In this regard, we face the challenge of limited availability within the local market of appliances designed to operate on DC.

For the power conversion process, high efficiency appliances based on switched power supplies have been developed. On the other hand, the first phase of operation of a switching power supply consists of the rectification or AC/DC conversion process for the operation of its internal components. This phase is key in the selection criteria of most household appliances, so it facilitates its incorporation into a DCHN without or with slight adaptations. Taking into account the process of cooking food within the home, it is identified that the induction cooker satisfies the selection criteria for incorporation. The technical data of the selected induction stove corresponds to a power of 3600 watts, 120 VAC, 60 Hz and 4 burners with trade mark Sisolar, as it is shown in Figure 2. The incorporation of the induction stove is carried out without any modification and with the use of accessories such as plugs and usual contacts in AC systems.

For the lighting sector, LED lamps are incorporated, whose operation of its internal components is carried out with DC. Within the local market, the following LED lamp is selected with the following technical data such as a power of 30 watts, a voltage of 120 VAC and a frequency of 60 Hz.

Figure 2 Induction stove into DCHN
Source: (Cordova-Fajardo & Tututi Hernández)

It should be noted that its incorporation into the DCHN is carried out without any modification. The selected LED lamp is shown in Figure 3.

Figure 3 LED lamp working at 120 VCD
Source: (Cordova-Fajardo & Tututi Hernández)

Finally, a blender is incorporated into the DCHN in order to cover the need for food preparation. The technical data of the blender corresponds to an operating voltage of 120 VAC, with a power of 600 watts at a frequency of 60 Hz, which is shown in Figure 4.

The appliances aforementioned have been selected to be incorporated into the DCHN above described. The following section describes their behavior within the DCHN.

Behavior of Appliances within DCHN

This section describes the behavior of the appliances selected for incorporation into the DCHN. The energy consumption data collected for each appliance is presented in two stages.

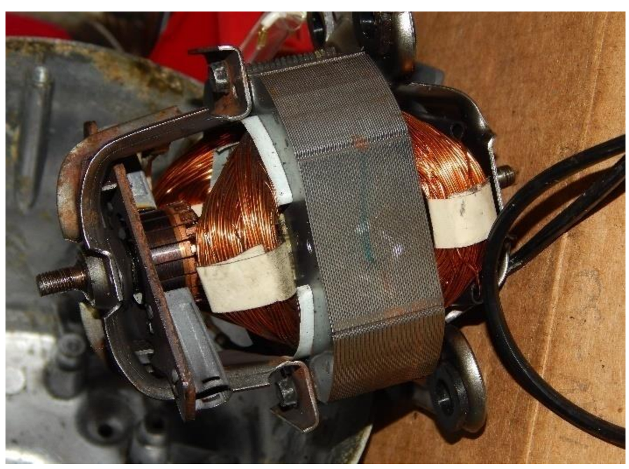

Figure 4 Blender motor
Source: (Cordova-Fajardo & Tututi Hernández)

ISSN-2523-2517

In the first stage, we obtain the measurement of the electric current at each appliance in the AC system with 120 VAC. At the second stage, we perform the measurements of the electric current, but now for the DCHN with nominal voltage of 120 VCD. In Table 1, it is shown the results for the electric current in each appliance.

Home appliance	CA	CD
Induction stove	10.8 A	9.1 A
Blender	2.4 A	2.7 A
LED lamp	450mA	380 mA

Table 1 Consumption of appliances in AC and DC regimens
Source: (Cordova-Fajardo & Tututi Hernández)

Let us stress that the electric accessories, such as plugs, switches and contacts were equally used in AC as in DC in the DCHN.

Results

The measurements for the induction stove in both AC and DC were obtained at the maximal power. However, this condition rarely occurs, and is of relatively short interval of time. That is to say, it happens when the end user wishes to quickly warm their meals. If the time interval of warming is large enough, it could burn the meal due to great quantity of energy supplied.

This condition could be demanding for the DCHN, for which results important its analysis. The resulting measurement of the electrical current consumption of the stove operating in DC within the DCHN is 15.74 % less with respect to system in AC. As far as the corresponding measurements in the blend is concerned, these results 12.5 % higher operating in the DCHN than in the AC system. For the LED lamp, we observed a diminishing of 15.55 % when the lamp operates in the DCHN.

Acknowledgements

This work has been partially supported by CIC-UMSNH and ITLAC.

Conclusions

The participation of different sectors (society, state, government or private initiative) involved in the energy market will favor the transition to sustainable systems.

The development and reduction of costs of energy storage devices will allow changes in the dynamics of the electric systems. These changes go from technical to economic aspects. The evolution of proposals such as DCHN than involve the use of sources of renewable energies and energy storage devices have increased the participation of end users and increased the awareness respect to their energy consumption style. Experimental data show an average decrease around of 15 % in the consumption of energy in a DCHN. Which is due to the reduction of stages in the energy conversion AC/DC. The generation and consumption of energy *in situ* avoids the transmission of energy at large distances with subsequent energy losses. Finally, in order to carry out the transition from AC to DC systems, it is necessary to implement technical standards to regulate the use of home appliances for to be manageable easily in both AC and DC. It is also necessary to define the level of the intensity of the voltage to operate a DCHN, to fix it as a standard.

References

AILee, G., & Tschudi, W. (18 de october de 2012). Edison Redux: 380 Vdc brings reliability and efficiency to sustainable data centers. *IEEE*, 50 - 59.

Barazarte, R. Y. (2013). La batalla de las corrientes: Edison, Tesla y el nacimiento del sistema de potencia. *Prisma Tecnologico, 4*(1), 51, 53.

Cordova-Fajardo, M. Á., & Tututi Hernández, E. S. (2019). Incorporating home appliances into a DC home nanogrid. *Journal of Physics: conference series, 1221*.

Moussa, S., Jebali-Ben Ghorbal, M., & Slama-Belkhodja, I. (2018). DC voltage level choice in residential remote area. *The 9th international renewable energy congress (IREC 2018).*

Szulecki, K., & Overland, I. (2020). Energy democracy as a process, an outcome and a goal: A conceptual review. *Energy Research & Social Science.*

Vitéz , B., & Lavrijssen , S. (2020). The Energy Transition: Democracy, Justice and Good Regulation of the Heat Market. *Energies*.

June 2021, Vol.5 No.14 14-19

Prototype simulation for the measurement of energy consumption in watts for alternating current systems

Simulación de prototipo para la medición del consumo de energía en watts para sistemas de corriente alterna

HERNÁNDEZ-LUNA, Aldo†*, CASTRO-JUÁREZ, Ana Magdalena, TORRES-JIMÉNEZ, Jacinto and HERNÁNDEZ-CABRERA, Hugo

Tecnológico Nacional de México/Instituto Tecnológico Superior de Huauchinango, Mexico.

ID 1st Author: *Aldo, Hernández-Luna* / **ORC ID**: 0000-0002-7717-5314, **CVU CONACYT ID**: 441305

ID 1st Co-author: *Ana Magdalena, Castro-Juárez* / **ORC ID**: 0000-0002-6499-6906, **CVU CONACYT ID**: 1116188

ID 2nd Co-author: *Jacinto, Torres-Jiménez* / **ORC ID**: 0000-0002-8006-6397, **CVU CONACYT ID**: 103469

ID 3rd Co-author: *Hugo, Hernández-Cabrera* / **ORC ID**: 0000-0002-7172-9734, **CVU CONACYT ID**: 368752

DOI: 10.35429/JEE.2021.14.14.19 Received January 20, 2021; Accepted June 30, 2021

Abstract

This research deals with the simulation of a prototype for the measurement of energy consumption in watts for alternating current systems, the purpose is to validate the proposed circuit for its implementation and in turn it provides a low-cost and easy-to-use measurement option for the public generally in their homes. The development of the prototype simulation will be carried out using the Arduino development environment with the components, Simulino Uno and the current sensor ACS712ELCTR-05B-T, from the Proteus Software. The current signal will be taken by the sensor to later pass it through a conditioning stage so that it is received by the microcontroller, where the programming will be carried out so that with the value obtained and the configuration of the voltage value, the power calculation in watts can be made, which will be displayed on a virtual monitor for viewing. This proposal seeks a device that performs the calculation of energy consumption in Watts that can lead the user to quantify and take better advantage of the use of electrical appliances or devices, and thus reduce the cost of their bill.

Simulation, Arduino, Energy consumption

Resumen

La presente investigación aborda la simulación de un prototipo para la medición del consumo de energía en Watts para sistemas de corriente alterna, la finalidad es validar el circuito propuesto para su implementación y a su vez este brinde una opción de medición de bajo costo y fácil uso para público en general en sus hogares. El desarrollo de la simulación del prototipo se realizará empleando el entorno de desarrollo Arduino con los componentes, Simulino Uno y el sensor de corriente ACS712ELCTR-05B-T, del Software Proteus. La señal de corriente la tomará el sensor para posteriormente pasarla por una etapa de acondicionamiento para que la reciba el microcontrolador, donde se realizará la programación para que con el valor obtenido y la configuración del valor de voltaje se pueda hacer el cálculo de potencia en Watts, el cual se desplegará en un monitor virtual para su visualización. La presente propuesta busca un dispositivo que realice el cálculo del consumo energético en Watts pueda llevar al usuario a cuantificar y aprovechar de una mejor manera el uso de aparatos o dispositivos eléctricos, y así disminuir el costo de su factura.

Simulación, Arduino, Consumo de energía

Citation: HERNÁNDEZ-LUNA, Aldo, CASTRO-JUÁREZ, Ana Magdalena, TORRES-JIMÉNEZ, Jacinto and HERNÁNDEZ-CABRERA, Hugo. Prototype simulation for the measurement of energy consumption in watts for alternating current systems. Journal Electrical Engineering. 2021. 5-14:14-19.

* Correspondence to Author (Email: aldo.hdz@huauchinango.tecnm.mx)
† Researcher contributing as first author.

Introduction

The awareness of electricity consumption within homes is still a culture with which many are not familiar since they do not have easy-to-interpret devices, it should be noted that currently the municipality of Huauchinango Puebla, where the research is developed, there is no regulation in the payment of electricity rates due to the extinction of the Luz y Fuerza del Centro company, which has generated an abandonment of the electrical infrastructure that in the medium term would cause it to collapse. This will lead to the regularization of electricity service payments and users will have to moderate and monitor their electricity consumption as well as visualize in real time how much they are spending per day, based on this data they will be able to manage and organize the use of electrical devices in order to have a benefit reflected in the billing of said service.

Due to the aforementioned, this research seeks to propose a feasible, low-cost and easy-to-use option for the measurement of energy consumption, which is why a simulation of the proposal is proposed at the beginning in order to later develop its implementation.

For the development of this work, a methodology consisting of 4 stages is used, which are listed below: 1) analysis of the components that will be used in the simulation, 2) design of the connection of the components that will form the electronic circuit, 3) programming the microcontroller in the arduino IDE indicating the tasks we want to do taking the reading of the sensors and the conditions of the environment to be programmed, 4) simulation of the proposed circuit using the Proteus software to analyze and validate its behavior.

Analysis

To carry out the simulation of energy consumption in Watts, it was essential to carry out the analysis and proposed the components that make up the circuit.

The design and simulation of the circuit are carried out in Proteus software, an application in which it is possible to design diagrams and simulate the code programmed in the microcontroller in real time. An alternating current source is used within the simulation and an alternating current lamp as load.

The central element for the control of the prototype is the Arduino Uno Module based on the ATmega328 microcontroller. For simulation purposes, the components of the Simulino Uno library are used and the Arduino IDE, the development environment of this microcontroller, to create the programming code.

Finally, the ACS712ELCTR-05B-T current sensor, this allows to measure the electrical intensity in both direct current and alternating current that makes it functional both in industrial applications, communication systems and commercial. It is based on the Hall effect, as the input current flows through the copper conductor and is detected by the sensor, it is converted into an output voltage that is proportional to the input current. Other advantages for which this sensor was used are: the different models for ranges 5, 20 and 30 A; the interconnection with Arduino and its affordable cost.

Design

To calculate the Watts consumed, it is first necessary to quantify the electric current that passes through the alternating current device of which we want to know the consumption in Watts for which a connection is established between it and the sensor, as shown in the figure 1.

Figure 1 Census of the current of the device to be measured
Source: Own elaboration

Once the current is obtained, it is received by the Arduino microcontroller where a programming code is used to calculate the power of the Watts consumed, the communication sequence is shown in figure 2.

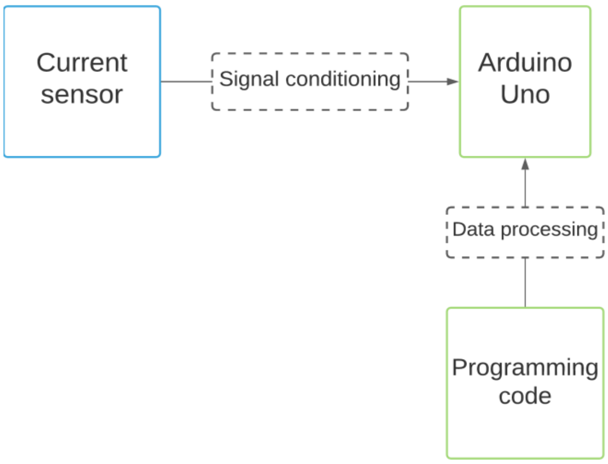

Figure 2 Data processing
Source; Own elaboration

Later this quantification of Watts will be shown by means of a virtual monitor. Prior to the physical assembly and simulation of said census, it is necessary to design the interconnection between the different devices that make up this measurement circuit, Figure 3 shows the general sequence of each element integrated into the circuit.

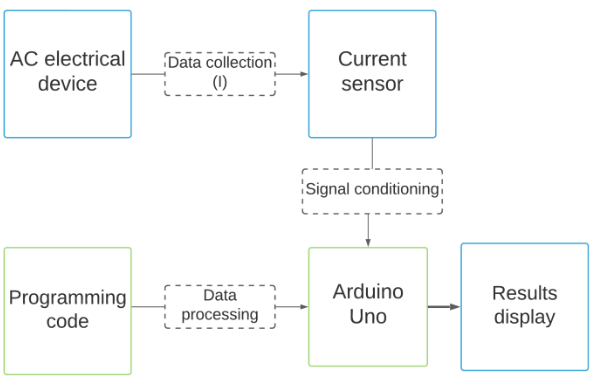

Figure 3 General sequence of the prototype to simulate
Source: Own elaboration

Programming

In the ARDUINO IDE program, the calculations for reading the analog input to the Arduino module were established, taking into consideration the specifications provided in the manufacturer's data sheet where it establishes that the current sensor under input intensity conditions equal to 0A delivers a voltage of 2.5 V and that from this increases proportionally according to the sensitivity (said sensitivity is established by the manufacturer for the case of the ACS712ELECTR-05B-T sensor is 185mV / A) we have that the relationship between the voltage and the current is a straight line where the slope is the sensitivity and the Y-intercept is 2.5 V, represented by the following equation:

$$V = mI + 2.5 \tag{1}$$

Where the slope *m* equals the sensitivity

To find the current from the sensor reading, it is done by means of the equations:

$$I = \frac{V - 2.5}{sensibilidad} \tag{2}$$

$$I = \left(5 * \frac{V_{\text{Censado}} - V_{entrada}}{1023}\right)\left(\frac{1000}{185}\right) \tag{3}$$

Where:

$$\left(5 * \frac{V_{\text{Censado}} - V_{entrada}}{1023}\right) \tag{4}$$

is the calculation to obtain the sensor voltage as a function of the input current, an average measurement of 1000 analog readings was made that subtracted from the input signal (analogRead A0) gives us a more precise value of the voltage tested as a function of the Input current. Incorporated into equation (3) we obtain the current reading.

Figure 4 shows the procedure to obtain the power in Watts, where the calculation for the peak values of the current wave was added in the programming since the current that we have previously found is oscillating at a frequency of 60 Hz.

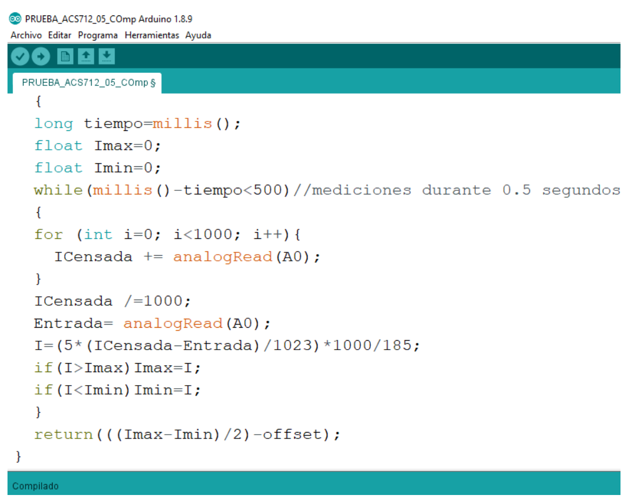

Figure 4 Programming code to obtain the effective current
Source: IDE ARDUINO

Once the peak current was obtained, the calculation of the effective current (RMS) and the code of the equation were added in the programming to calculate the power consumed in Watts. Likewise, as shown in figure 5, the serial.Print () commands are used to display on the virtual monitor the text indicating the parameters obtained as well as the total Watts consumed and serial.Println () to indicate the values to read and display.

Figure 5 Code to obtain the power consumed in Watts
Source: IDE ARDUINO

Simulation

Based on the general sequence of the prototype to be simulated, the electronic diagram and the electrical connections between each component of the prototype are designed. As previously mentioned, the software used for the simulation was Proteus, in which before starting to add any component it was necessary to make some adjustments such as downloading and adding the SIMULINO libraries corresponding to the Arduino module. Once added in the Proteus software, the electrical components that are part of the circuit were selected and configured as shown in figures 6 and 7, these elements are:

- Sensor ACS712ELCTR-05B-T.
- 0.1µF and 1nF capacitors.
- + 5V power supply for the sensor.
- Arduino module.
- AC source set to 127 V, 60 Hz.
- To represent the load, a lamp with the following characteristics was selected; 127 V, 200 Ω.
- Virtual terminal for visualization of results.

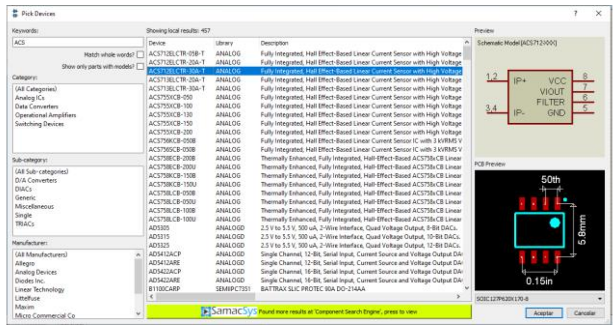

Figure 6 Search and selection of components
Source: Proteus software

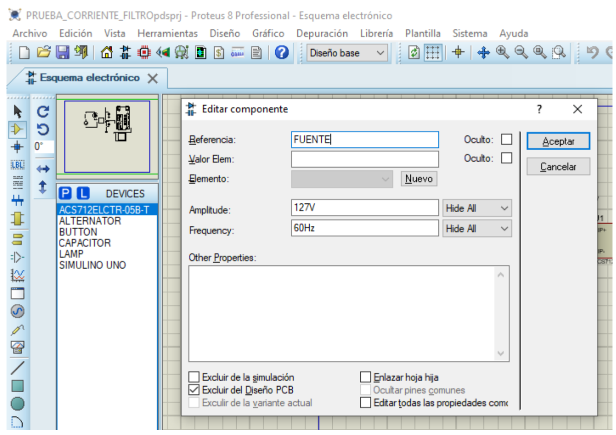

Figure 7 Element configuration
Source: Proteus software

For the configuration of the sensor connection, figure 8, two filters are added in order to attenuate the noise since this sensor generates an analog output signal (Vout) that varies linearly with the sampled AC. Two capacitors are added to the filter, with values (0.1µF and 1nF) for a typical application recommended by the manufacturer's data sheet.

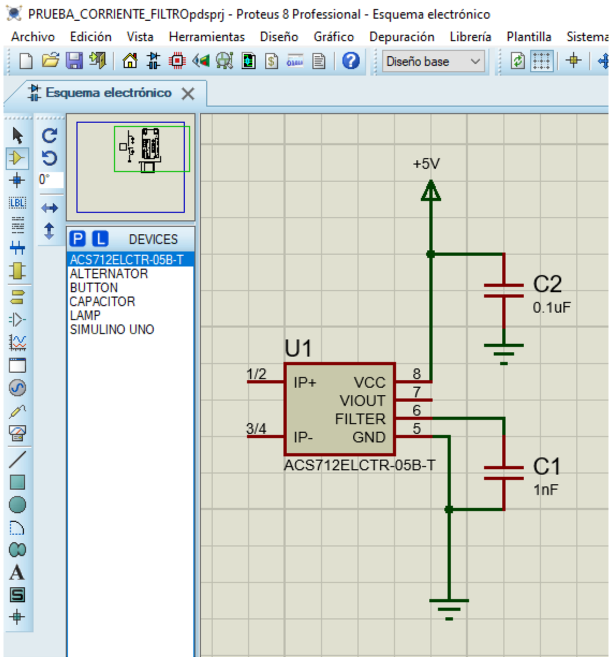

Figure 8 Sensor configuration
Source: Proteus software

Finally, figure 9 shows how all the elements are integrated after each one of them has been configured. In this last figure, the virtual terminal for displaying results can also be seen already integrated.

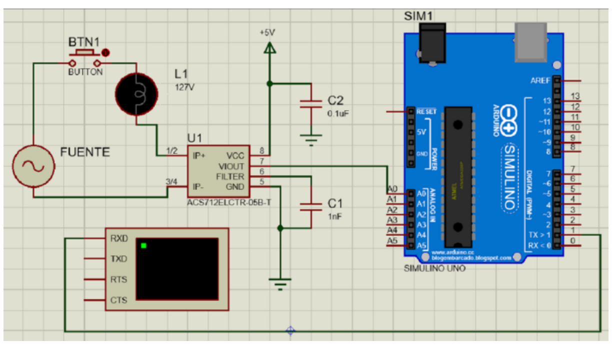

Figure 9 General circuit
Source: Proteus software

When performing the current monitoring simulation to calculate the power consumed by the circuit, the .HEX file generated in the Arduino IDE was loaded to the Arduino module (Simulino) where the program was made and compiled with the code designed to perform the Necessary calculations and obtain the peak current (Ip), effective current (IRMS) and finally the calculation of the power consumed in Watts.

In the simulation stage, the structure and connection between each of the modules used in the system is defined. With this stage it is possible to verify that the designed circuit works correctly as expected and can be implemented.

Results

The design of the final circuit to carry out the simulation in the Proteus Software is as shown in figure 10, in the virtual monitor of the simulation the peak and effective values (RMS) of the current are obtained as well as the value corresponding to the power. In addition to displaying the current and voltage values sent from the sensor to the arduino microcontroller.

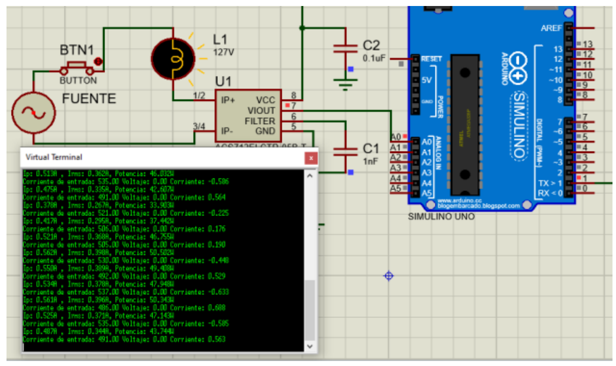

Figure 10 Circuit simulation
Source: Proteus software

Table 1 shows different values of effective current measured in amperes (Irms), the power measured in Watts (Pmed) and the calculated power data (Pcal) are added. The Pmed represents the measurement of the Watts consumed that are displayed in the virtual terminal of the simulator, on the other hand, the Pcal is determined by multiplying the effective current measured Irms by the fixed voltage of 127 V, this to delimit the error between these and validate the values measured power. The% error is determined with the difference of the Pmed and Pcal.

I_{rms} (A)	P_{med} (W)	P_{cal} (W)	%error
0.604	76.710	76.708	0.0026
0.609	77.381	77.343	0.0491
0.610	77.407	77.470	0.0813
0.613	77.888	77.851	0.0475
0.614	77.916	77.978	0.0795
0.617	78.374	78.359	0.0191
0.618	78.427	78.486	0.0752
0.622	78.987	78.994	0.0089
0.623	79.162	79.121	0.0518
0.626	79.492	79.502	0.0126
0.627	79.586	79.629	0.0540
0.628	79.721	79.756	0.0439
0.632	80.290	80.264	0.0324
0.633	80.452	80.391	0.0759
0.634	80.577	80.518	0.0733
0.635	80.685	80.645	0.0496
0.636	80.784	80.772	0.0149
0.642	81.560	81.534	0.0319
0.643	81.654	81.661	0.0086
0.644	81.771	81.788	0.0208
0.652	82.827	82.804	0.0278
0.653	82.939	82.931	0.0096

Table 1 Values to delimit the% error between measured and calculated power
Source: Own elaboration

The low percentage of error and the minimum difference between the measured and calculated power can be seen in Graphic 1. This difference is due to the analog signal that the current sensor is detecting and that reflects at the output a measurement proportional to the degree of sensitivity of it.

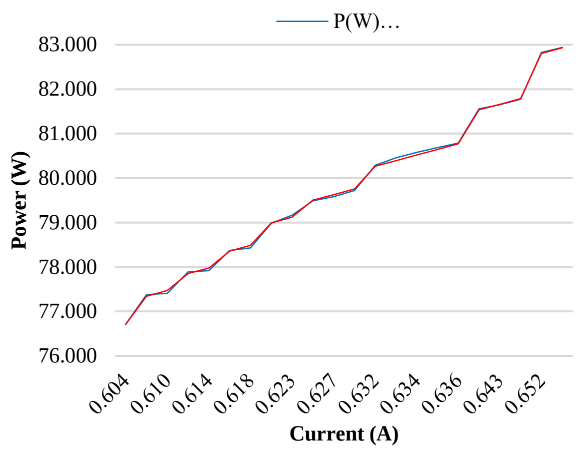

Graphic 1 Comparison between measured and calculated power
Source: Own elaboration

Gratitude

The authors wish to express their gratitude to the Postgraduate program, Master in Information Technology, of the Instituto Tecnológico Superior de Huauchinango for the support and facilities for the development of this work.

Conclusions

This article presents the simulation of a prototype for measuring energy consumption in Watts for alternating current systems. The simulation allows us to validate the electronic circuit proposal for its implementation, and thus generate an attractive device for the general public since it would be accessible in cost and easy to use.

The proposal handles a current sensor, the voltage is specified from the programming this in order to find a functional circuit and with a simple structure in addition to complying with the voltage tolerance of ± 10% established by the Federal Electricity Commission, current and sole electricity marketer in Mexico. With both parameters delimited, the microcontroller calculates the power in Watts, to later print it on the virtual monitor.

It should be noted that to carry out the implementation of a system it is always necessary to carry out a simulation that can guarantee its proper functioning.

References

Guerrero Quichiz, G. M. (2007). Diseño e implementación de un sistema de control digital con conexión a redes de datos para medición de parámetros eléctricos (Tesis para optar el título de ingeniero electrónico). Pontificia Universidad Católica del Perú Facultad de Ciencias e Ingeniería.

Mora-Martínez, A. S., Villalvazo-Laureano, E., & Jiménez-Betancourt, R. O. (2020, 1 enero). Medidor de parámetros eléctricos con visualización remota. Revista de Aplicaciones de la Ingeniería, 7(22), 23-28. https://doi.org/10.35429/JEA.2020.22.7.23.28]

Vázquez Palma, M. G., Flores Figueroa, J., Soto Rodríguez, M., & Romero Ochoa, M. A. (2018, junio). Diseño de un medidor de energía eléctrica bidireccional y monitoreado mediante aplicación móvil. Revista Iberoamericana de las Ciencias Computacionales e informática, 7(13), 5-30. https://doi.org/1 Arduino (2020).

Arduino Products. Retrieved from: https://www.arduino.cc/en/Main/Products

Rosales, M. (2020). Concepto de Programación. Retrieved from: https://www.zonaeconomica.com/conceptoprogramacion. 0.23913/reci.v7i14.84

Sistema de infraestructura avanzada de medición AMI, CFE G0100-05.

Article

Journal Electrical Engineering

June 2021, Vol.5 No.14 20-31

Analysis of power quality in photovoltaic systems interconnected to the grid

Análisis de calidad de la energía en sistemas fotovoltaicos interconectados a la red

DIBENE-ARRIOLA, Luis Martin†*´, FLETES-CAMACHO, Noé Guadalupe´, PAREDES-VAZQUEZ, César Paul´ and MARROQUÍN-DE JESÚS, Ángel´´

´Universidad Tecnológica de Bahía de Banderas, Engineering Division Renewable Energies and Industrial Maintenance, Nayarit 63732, Mexico.
´´Universidad Tecnológica de San Juan del Río, Chemistry and Renewable Energy Division, Querétaro, Mexico.

ID 1st Author: *Luis Martin, Dibene-Arriola* / **ORC ID:** 0000-0002-1906-4528, **CVU CONACYT ID:** 412156

ID 1st Co-author: *Noé Guadalupe, Fletes-Camacho* / **ORC ID:** 0000-0002-2435-6971. **Researcher Thomson ID:** U-9488-2018. **arXiv Author ID:** 2839471

ID 2nd Co-author: *César Paul, Paredes-Vazquez* / **ORC ID:** 0000-0002-4408-9487, **arXiv Author ID:** 284265, CVU CONACYT ID: 890844

ID 3rd Co-author: *Ángel, Marroquín-De Jesús* / **ORC ID:** 0000-0001-7425-0625, **CVU CONACYT ID:** 81204

DOI: 10.35429/JEE.2021.14.20.31 Received January 25, 2021; Accepted June 30, 2021

Abstract

A lot of authors are concluded that photovoltaic systems distort the waveform of voltage and current, the evaluation of these distortion indices is carried out in accordance with IEEE Std 519-2014, equipment sensitive to variations in the voltage wave, are affected in their operation, causing a rise in temperature, a decrease in speed in rotating machines, among others, these variations are accentuated by low irradiance values. In this work, the results of the online monitoring of electrical parameters are shown, when connecting a network analyzer Hioki® model PQ3198, class A, in the terminals of the alternating current side of the Fronius® inverter, SYMO 10.0-3 208 / 240V of a 10 kWp commercial photovoltaic system and a GOODWE® inverter, model GW-2000-NS with 220 output voltage in a 2 kWp home photovoltaic system; The measurement period was one week, the analyzer was programmed to sample every 5 minutes. Finding effects on voltage and current harmonics greater than 5% established in the IEEE 1100-1999 standard, but less than 10% established in the Mexican legal framework, in accordance with CFE Specification L0000-45 "Permissible deviations in waveforms of voltage and current in the supply and consumption of electrical energy" the values of the harmonic distortion indices have a variation of 8%.

Photovoltaic systems, Disturbances, Power quality

Resumen

Diversos autores concluyen que los sistemas fotovoltaicos distorsionan la forma de onda de voltaje y corriente, la evaluación de estos índices de distorsión se realiza de conformidad con el IEEE Std 519-2014, equipos sensibles a variaciones en la onda de voltaje, son afectados en su funcionamiento, ocasionando elevación de temperatura, disminución de la velocidad en máquinas rotativas, entre otras, estas variaciones se acentúan más ante bajos valores de irradiancia. En el presente trabajo se muestran los resultados del monitoreo en línea de parámetros eléctricos, al conectar un analizador de redes Marca Hioki® modelo PQ3198, clase A, en las terminales del lado de corriente alterna del inversor Fronius®, SYMO 10.0-3 208/240V de un sistema fotovoltaico comercial de 10 kWp y de un inversor GOODWE®, modelo GW-2000-NS de 220 volts de salida en un sistema fotovoltaico doméstico de 2 kWp; El período de medición fue de una semana, se programó el analizador para que realizará un muestreo cada 5 minutos. Encontrándose afectaciones de voltaje y armónicos de corriente mayores al 5% establecidas en el estándar IEEE 1100-1999, pero menores al 10% establecido en el marco legal mexicano, de conformidad con la Especificación CFE L0000-45 "Desviaciones permisibles en las formas de onda de tensión y corriente en el suministro y consumo de energía eléctrica" los valores de los índices de distorsión armónica tienen una variación del 8%.

Sistemas fotovoltaicos, Perturbaciones, Calidad de la energía

Citation: DIBENE-ARRIOLA, Luis Martin, FLETES-CAMACHO, Noé Guadalupe, PAREDES-VAZQUEZ, César Paul and MARROQUÍN-DE JESÚS, Ángel. Analysis of power quality in photovoltaic systems interconnected to the grid. Journal Electrical Engineering. 2021. 5-14:20-31.

* Correspondence to Author (Email: ldibene@utbb.edu.mx)
† Researcher contributing as first author.

Introduction

This topic arises from an investigation about greenhouse gas (GHG) emissions from beach hotels; when in an interview with a hotel maintenance manager, he states that he is not interested in the use of Photovoltaic Systems (PV) to reduce GHG emissions into the atmosphere since, according to him, PV burn the electronic cards of the equipment laundry and air conditioning by affecting the quality of electrical energy.

Electricity consumption in hotels is generally used for lighting, use of elevators, water pumping, air conditioning, electrical kitchen machinery, kitchen equipment, electric heat pumps, etc. Additionally, hotels consume some fuel, such as LP gas, diesel or natural gas, for the generation of sanitary hot water, pool water heating and for cooking (SEMARNAT, 2020).

Electronic equipment is damaged by any of the following causes: Overvoltages, overcurrents (overloads, short circuits and ground faults), electromagnetic and electrostatic interference, contamination, heating and by problems associated with power quality, such as resonance (Ruelas, 2021). This work will try to answer the question: Do photovoltaic systems cause damage to the electronic boards of air conditioning and laundry equipment? The afore mentioned, he worried us since it is currently considered very important to reduce these emissions and that type of comments can influence the interest in the VFs of other hotels.

Background:

(Favuzza, Graditi, Spertino, & Vitale, 2004) They investigated the impact of SFVs on the quality of the power of the network. Their results show that the level of harmonic distortion at the point of common coupling (PCC) is comparable to levels of distribution networks without distributed generation and that there are no critical consequences in terms of voltage distortion at the PCC. The results obtained show that the impact of photovoltaic inverters on the quality of the energy of the network depends on the impedance of the electrical network and that investors with different types, connected to the urban network, have indicated a very similar behavior.

On the other hand, (Hernández & Medina, 2006) state that the fundamental aspects of supply quality that must be evaluated in the PCC are: voltage and frequency variation, voltage dips and overvoltage intervals, flicker, unbalance, harmonic distortion, power factor and reactive power. They indicate that photovoltaic generators that have inverters with PWM technology inject minimal harmonic currents into the grid with little effect on supply quality and that flickers and voltage imbalances are comparable to those existing in the electricity grid (low voltage) without photovoltaic generation.

Finally, they conclude that the photovoltaic inverter plays a fundamental role in the operation of the photovoltaic generator in relation to the quality of supply parameters. (González-Castrillo, Romero-Cadaval, González-Romera, Barrero-González, & Guerrero-Martínez, 2007), show results of the measurement of power quality parameters carried out in a rural distribution network in two periods of time, previous and after the connection to the line of a photovoltaic plant and also present the same parameters registered in the PCC and recognize a slight impact of the photovoltaic subsystems on the harmonic voltage distortion. (Patsalides, et al., 2007) considered 14 different grid-connected photovoltaic systems in Cyprus and conducted online monitoring of electrical parameters.

They found that low solar irradiance has a significant impact on the quality of the output power of the photovoltaic system. The electrical parameters recorded were: active power, reactive power, voltage and current for each harmonic frequency. They also measured power factor and total harmonic distortion for voltage and current for two weeks. They found that the power factor is greater than 80% for irradiances greater than 300 W/m^2 and falls below that value with lower irradiances. That the reactive power varies significantly during the day of and that the rapid variations of the reactive power supplied by the photovoltaic systems, assuming very high densities of such systems, can cause a fast switching of the capacitor and that due to these oscillations and transients of voltage can occur with unpredictable amplitude and duration.

ISSN-2523-2517

That these transients can cause failures in sensitive electronic equipment or minimize the life expectancy of network elements, if the amplitude of a transient exceeds the limits of the IEEE Std 1159-1995 (R2001) Recommended Practice for Monitoring Electric Power Quality, the Limit values for transients are (Table 2):

IEEE
Std 1159-1995

IEEE RECOMMENDED PRACTICE FOR

Table 2—Categories and typical characteristics of power system electromagnetic phenomena

Categories	Typical spectral content	Typical duration	Typical voltage magnitude
1.0 Transients			
1.1 Impulsive			
1.1.1 Nanosecond	5 ns rise	< 50 ns	
1.1.2 Microsecond	1 μs rise	50 ns–1 ms	
1.1.3 Millisecond	0.1 ms rise	> 1 ms	
1.2 Oscillatory			
1.2.1 Low frequency	< 5 kHz	0.3–50 ms	0–4 pu
1.2.2 Medium frequency	5–500 kHz	20 μs	0–8 pu
1.2.3 High frequency	0.5–5 MHz	5 μs	0–4 pu

Therefore, it is desirable to reduce the existence of such transients. Finally, they found that current harmonics are very sensitive to changes in incident radiation. (Çelebi & Çolak, 2011) investigated the effects of harmonic distortion in electrical networks, depending on the location and number of photovoltaic systems, using the simulation program Pspice®.

They found that harmonic currents generated by photovoltaic systems can degrade the quality of the electrical grid and alter the performance of other electrical equipment. According to the simulation results, the harmonic distortion generated by the photovoltaic generators is below the standards in a distribution network that only has domestic loads and that if the photovoltaic generators are located close to the transformer, the harmonic distortion becomes even lower.

In addition, the installation of photovoltaic systems close to the transformer helps to control the increase in voltage in the distribution lines. They found that the inverters used in the simulation circuit affect the harmonic levels, so their quality properties are important for the network. (González, Romero-Cadaval, E., & Guerrero, 2011) carried out measurements on power quality parameters (PQ) carried out in a radial distribution network in two periods of time, before and after connecting a photovoltaic plant to the network at the common coupling point of the grid and the photovoltaic plant.

Some measured values are compared to the limits established in IEEE Std 519-2014. The measurements carried out in the network showed that the insertion of the photovoltaic plant causes changes in the measured quality parameters and operational characteristics that do not seriously affect the operation of the network. (Bouchakour, Chouder, Cherfa, Abdeladim, & Kerkouche, 2012) analyzed and evaluated the measurements of the photovoltaic array under test to observe the general effect of solar irradiance on the operation of the systems connected to the grid under test.

They found that solar irradiance has a significant impact on the quality of the output power of the photovoltaic system as the active power and power factor go down, while the reactive power goes up. In addition, a TRMS voltage drop is observed in the range of 210-220V, contrary to that observed for the case of average irradiance in the range of 220-230V. Gallo et al. (2013) carry out an analysis of the common indices of energy quality in steady and transient state, both on the AC and DC sides from experimentally recorded data in a medium-scale photovoltaic system that is connected to the grid, in order to understand and explore the nature of the electricity generation patterns of photovoltaic plants.

They find that the steady state indices during a sunny day are: plants at fundamental frequency behave as an ideal source with an almost unity power factor. That the total harmonic distortion of voltage (THDV) as a function of the active power is practically uncorrelated with the output power of the system and that the total harmonic distortion of current (THDI) is high for low active power, since the inverter does not work in its nominal operating conditions, generating a highly distorted current waveform at certain times of the day (for example, at sunrise and sunset). That the voltage imbalance is not correlated with the active power. That the maximum and average values of the groups of voltage and current harmonics at low frequency (50-2500 Hz) measured throughout the day have notable amplitudes in the 3rd, 5th and 11th order. That the eleventh harmonic has a high value in both voltage and current and that it could provide useful information about the state of the network. (Lu, Wang, Ke, Chang, & Yang, 2014) found that the power quality of an PV system complies with the Taiwan Power Company grid code.

During one-week electrical parameter measurements were made on a connected 70.38 kW SFV at the National University of Science and Technology Peng-Hu, Taiwan and the recorded results include three-phase voltages, currents, active power, reactive power, power factor, frequency, current harmonics, voltage flickers and voltage variations. (Misak, Prokop, & Bilik, 2014) mention that energy quality problems may arise due to the use of renewable sources in active distribution networks and that these problems are caused by the decrease in the short-circuit power of local renewable sources, the stochastic supply of electrical energy from renewable sources and the operation of the active distribution network in autonomous mode without connection to the external distribution system. In the case of these conditions, the mutual interference between sources and loads is relevant and the quality parameters of electrical energy can be exceeded (Niitsoo, Jarkovoi, Taklaja, Klüss, & Palu, 2015) analyze the harmonic content of photovoltaic generation and the influence on power quality indicators in residential distribution networks. They found moderate additional harmonic distortion in the residential load current and voltage distortion in the substation busbar when photovoltaic panels were added. (Caballero, Cortez, Muñoz, & Castañeda, 2016) mention that the biggest problem in photovoltaic supply is harmonics, due to the waveform delivered by the inverter. That to solve harmonic problems in the network, signal conditioners are used, ranging from tuned passive filters to active filters.

That the former is cheaper, but their selectivity does not allow them to compensate beyond their tuned frequency, while the active filters present a dynamic solution that adjusts to the compensation needs. That they used the active series filter for its main objective of eliminating voltage harmonics, which achieves that both the current and the voltage are sinusoidal. As a result of the implementation of the active filter, the reduction of the harmonic content from 48.3% originally to 2.61% was demonstrated in simulation (this harmonic content must be current), thus complying with the IEEE 519-1992 and CFE L0000- 45 Mexican. (Durán, Raggio, Socolovsky, Videla, & Plá, 2016) analyze energy quality: (i) at the connection point of a 40 kWp PV system installed in the Scientific and Technological Pole, and (ii) in one of the the electrical circuits of a single-family home.

They found that the harmonic components of current injected into the network by the SFV are clearly below the limits established by the IEC 61000-3-2 standard and that the harmonic components of current emitted by household appliances are significantly higher than the harmonics injected by a typical power PV inverter for a single-family home so the connection of PV systems to the electrical grid does not affect the quality of service in terms of harmonic distortion. (Afonso, de Arruda Bitencourt, Fortes, Gomes, & Maciel, 2018) analyzed the harmonics generated in a system when there are different levels of photovoltaic solar generation penetration. They simulated a real system in the city of Buzios (Brazil) in the HarmZs® program with measured values from existing panels and evaluated the total harmonic voltage distortion.

They observed that in the scenarios with massive penetration of photovoltaic generators, the established limits were violated, so the insertion of new (small) renewable sources connected to the grid must be discussed in the context of energy quality to avoid large distortions in the electrical systems so that they are adequate and comply with the existing regulations for energy distribution. (Spertino, et al., 2018) mention that in the case of PV systems, harmonic injection and unbalance are due to pulse width modulation (PWM) switched transistors inside the converters, therefore quantified the impact of harmonic distortion on disequilibrium. They then tested a photovoltaic system with a multi-inverter configuration and made power quality measurements of the worst and best converters to finally compare with the overall power quality measurements of all inverters.

From the review of publications on the subject, the following results were found:

1. Publications that mention that photovoltaic systems do not significantly affect the quality of electrical energy at the PCC and that the level of harmonic distortion is comparable to the levels of distribution networks without distributed generation and that there are no critical consequences in terms of distortion in the PCC (Favuzza, Graditi, Spertino, & Vitale, 2004), (Hernández & Medina, 2006), (González-Castrillo, Romero-Cadaval, González-Romera, Barrero-González, & Guerrero-Martínez, 2007), (González, Romero-Cadaval, E., & Guerrero, 2011), (Lu, Wang, Ke, Chang, & Yang, 2014), (Niitsoo, Jarkovoi, Taklaja, Klüss, & Palu, 2015) y (Durán, Raggio, Socolovsky, Videla, & Plá, 2016).

2. Publications that state that the harmonic currents generated by photovoltaic systems can degrade the power quality grid and alter the performance of other electrical equipment and that the inverters used affect harmonic levels, so their quality properties are important for the network since the quality parameters of the electrical energy can be exceeded. (Çelebi & Çolak, 2011), (Misak, Prokop, & Bilik, 2014) y (Afonso, de Arruda Bitencourt, Fortes, Gomes, & Maciel, 2018).

3. Publications that mention that low solar irradiance has a significant impact on the quality of the output energy of the photovoltaic system (Patsalides, y otros, 2007), (Bouchakour, Chouder, Cherfa, Abdeladim, & Kerkouche, 2012) y (Gallo, Landi, Luiso, & Edoardo, 2013), a situation that occurs at dawn and dusk of the day.

4. That the biggest problem in the photovoltaic supply are harmonics, due to the waveform delivered by the inverter. That to solve the harmonic problems in the network, signal conditioners are used, ranging from tuned passive filters to active filters (Caballero, Cortez, Muñoz, & Castañeda, 2016).

In addition to the above results, the fundamental aspects of supply quality that must be evaluated in the PCC are: voltage and frequency variation, voltage dips and overvoltage intervals, flicker, unbalance, harmonic distortion, power factor and reactive energy (Hernández & Medina, 2006).

It is clear from the previous review that there are different results in the studies about the effect on the quality of electrical energy when using VFS. Therefore, this study seeks to determine for a 2 kW domestic PV system installation and a 10 kW commercial one how the power quality is affected and if this affectation can damage the electronic boards of the devices of a given installation.

Materials and methods

Measurements were made at a 10kWp commercial PV system and also at a 2 kWp domestic SFV; located in Puerto Vallarta, Jalisco and Nuevo Vallarta, Nayarit respectively, both interconnected to the grid of the basic service provider under the Net Metering contract scheme, Net Metering or Net Metering is a form of billing in which the consumer generates and consumes electrical energy in the same supply contract. The systems present differences in marks, inclinations, orientations and the electrical installation. Even the network, although it can be interpreted that it depends on the same source of public generation, the network behaves with different parameters adding that the commercial system corresponds to a three-phase system and the residential one to a single-phase 2-phase system.

The only common thing is that the two systems were monitored by the same instrument, a Hioki® model PQ3198 power quality analyzer, current sensors calibrated at 500A for the commercial system and 50A for the residential system and a range of 5-minute record for both systems, it is important to mention that the equipment used for the measurements is calibrated by the company Welsh Instrumentation Electronic Measurement and Control Equipment. Considering the above, the two monitoring have different dates and times, but even so the results can be conclusive.

The characteristics of both systems are shown in tables 1 and 2 below:

Capacity	10 kWp
Number of panels	40
Peak power of each panel	265 W
Panel brand	SOLAREVER®
Panels model	SE-156*156-P-60
Inversor brand	Fronius®
Inverter model	SYMO 10.0-3 208/240
Maximum power output	13 kW

Table 1 10 kWp photovoltaic system

Capacity	2 kWp
Number of panels	6
Peak power of each panel	330 W
Panel brand	Risen Solar Technology
Panels model	RSM72-6-330P
Inversor brand	GOODWE
Inverter model	GW-2000-NS
Maximum power output	2.6 kW

Table 2 2 kWp photovoltaic system

The following figures 1 and 2 show the arrangement of both systems:

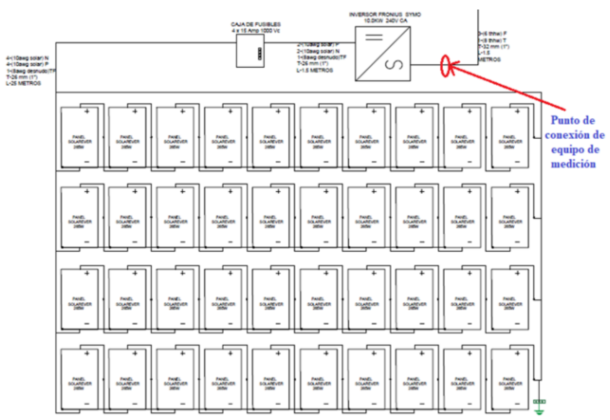

Figure 1 10 kWp Commercial PV system connection diagram

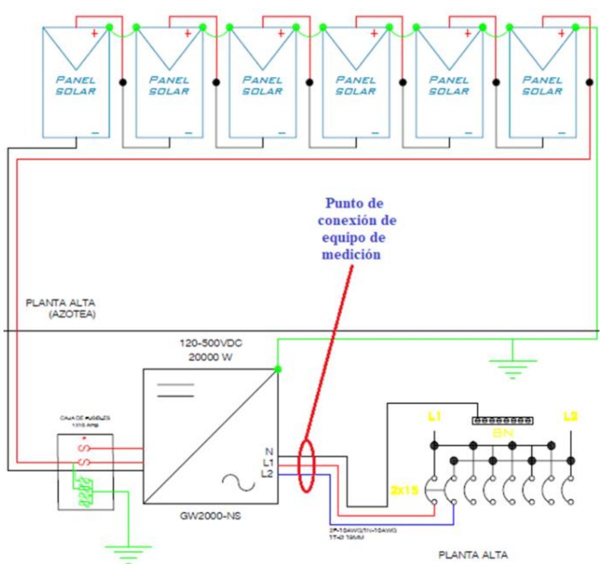

Figure 2 2 kWp domestic PV system connection diagram

Results

10 kWp commercial photovoltaic system

The analysis of the electrical monitoring carried out at the facilities of the company construction materials La Vena S.A. de C.V., located in Puerto Vallarta, Jalisco. The electrical installation is of the commercial type, designed for office equipment, home and power equipment for a semi-automatic block machine. It presents a main board of 20 branch circuits 120/240 V, 3 phases – 4 wires (3F-4H) Model QO1201125 Square D®, it houses inside: 15 thermomagnetic switches of 1 x 20 A, 1 thermomagnetic switch of 2 x 20 A and a 3 x 50 Amp thermomagnetic switch, 4 secondary load centers; offices, block, large house and office expansion.

In the office charging center is the interconnection point of a 10 kWp PV system, at that point the Hioki® power quality analyzer model PQ3198, class A was connected to monitor the electrical parameters, in the period of time from November 4 to 11, 2020.

2 kWp residential photovoltaic system

The photovoltaic system supplies electricity to a house of approximately 98 m^2 of construction, located on Valle del Bambú street number 305 of the Los Encantos neighborhood in Nuevo Vallarta, Nayarit. The house has; three bedrooms, two bathrooms upstairs, living room, kitchen, dining room and service yard. Unlike the commercial service, this has a photovoltaic system in the same scheme (Net metering) but with a lower power system, 2kWp. The system's interconnection point is located in the only load center, it receives a power supply from the basic service provider 2 phase-3-wire (3F-3H) 220 V. At this point, the Hioki® power quality analyzer model PQ3198, class A was connected to monitor electrical parameters, in the period of time from December 3 to 11, 2020.

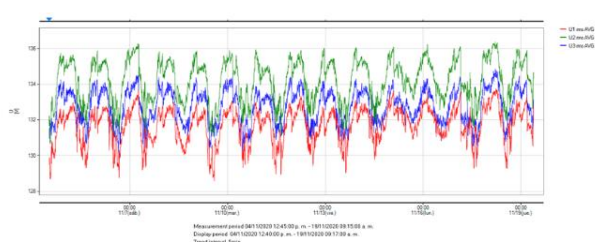

Figure 3 10 kWp PV system voltage profile graph

In general, the 3 phases presented instantaneous variations (Figure 3). The values were compared with the IEEE 1100-1999 standard, variation not greater than 5% and the regulation of the law of the public electricity service, which in its chapter V article 18 indicates that the supplier must offer and maintain the service in the form of Alternating current in one, two or three phases, at high, medium or low voltages, available in the area in question, observing the following: I. II. That the frequency is 60 Hertz, with a tolerance of 0.8 percent more or less, and that the tolerances on high, medium or low voltage do not exceed ten percent more or less and tend to be reduced progressively.

Phase	Nominal phase-to-neutral voltage	Phase-to-neutral voltage (V) Mínimum	Average	Maximum	Limits	IEEE Std 1100-1999
1	127 V	130.80	131.71	131.97	± 5%	Complies
2	127 V	133.45	134.22	134.55		Complies
3	127 V	132.09	132.77	133.11		Complies

Table 3 Measurement values obtained compared to IEEE Std 1100-1999

Phase 1 presents an average 3.76% above the nominal value, phase 2 presents an average of 5.61% above the nominal value and phase 3 presents an average value of 4.59% above the nominal value (Table 3).

Current profile

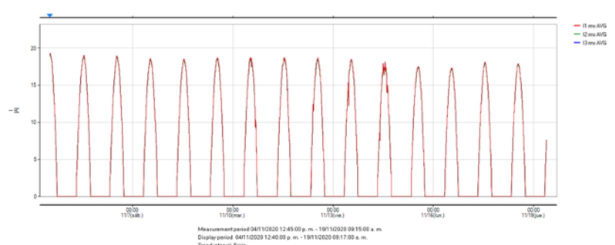

Figure 4 Graph of current profile in PV system of 10 kWp

In general, the 3 phases present a balanced behavior, registering average values of 19.5 A per phase at 1:00 p.m. The variation in amperage is not periodic and is caused by variations in solar irradiance in the solar panels. Throughout the monitoring period, there were no other disturbances that affect the quality of energy due to the effect of the current.

Power profile

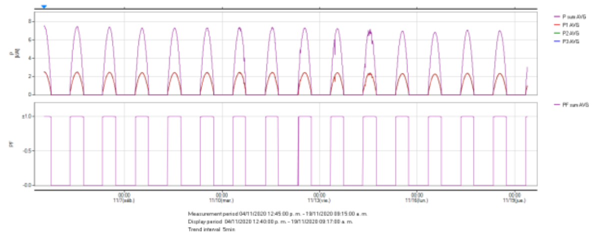

Figure 5 Graph of the power profile in PV system of 10 kWp

In general, in figure 5, the 3 phases presented a maximum individual real power (kW) of 2.4 kW and a total of 7.31 kW. The values are reasonable considering that it has an installed photovoltaic capacity of 10 kWp. Since it is not an efficiency study, the comparative alternating current power versus photovoltaic power is not made.

The lower part of the graph shows the behavior of the power factor throughout the measurement period. Due to the type of system in question, electricity generation from a linear signal in this case, the average value of the power factor throughout the measurement time was 0.99. Measurements were made with original factory settings (Table 4).

Power	Power values Minimum	Average	Maximum	Inverter power in kWp
Apparent (kVA)	7.53	7.56	7.59	
Real (kW)	7.52	7.55	7.57	13
Reactive (kVAR)	-0.75	-0.36	0.51	

Table 4 Measurement values obtained

Harmonic component profile of voltage and current

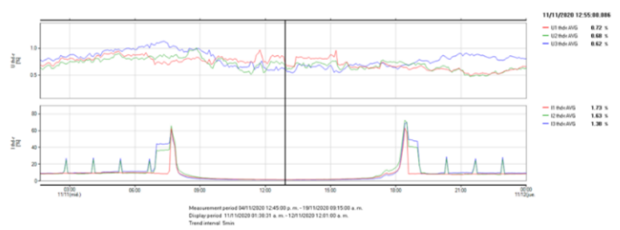

Figure 6 Graph of voltage and current profile in PV system of 10 kWp

ISSN-2523-2517

Figure 6 shows the behavior of the inverter, with early morning being the left side and nighttime being the right side, the upper part shows THDv and lower part of current THDi. In graph 4 it can be seen that during the operation of the inverter it shows average THDi values of 1.6% in each phase and a practically periodic voltage harmonic distortion behavior of 0.6% of THDv. This is due to the fact that all the time the inverter is receiving a potential difference at the measurement point and this will be the value of the grid, as opposed to the current. This only shows reading when the inverter is injecting energy into the grid and is capable of controlling the harmonic contribution, at night, as it does not have a generation and the equipment goes to "rest state" there is no current circulation so that the reading you have may be due to interference or noise due to a zero value or milliamp readings. The manufacturer of the inverter in its technical sheet shows a THDv of 1.5%, according to the registered data they are under that margin.

For THDv, the maximum value reached in the measurements is approximately 1.2%, comparing the values with table 1 of IEEE Std 519-2014, it is observed that it complies with this total harmonic distortion index in voltage.

Table 1—Voltage distortion limits

Bus voltage V at PCC	Individual harmonic (%)	Total harmonic distortion THD (%)
$V \leq 1.0$ kV	5.0	8.0
1 kV < $V \leq 69$ kV	3.0	5.0
69 kV < $V \leq 161$ kV	1.5	2.5
161 kV < V	1.0	1.5[a]

[a]High-voltage systems can have up to 2.0% THD where the cause is an HVDC terminal whose effects will have attenuated at points in the network where future users may be connected.

Source: https://edisciplinas.usp.br/pluginfile.php/1589263/mod_resource/content/1/IEEE%20Std%20519-2014.pdf

Phase	THDV Máx.	Maximum limit (%)	Std. IEEE 519-2014
1	0.69	8%	Complies
2	0.66		Complies
3	0.55		Complies

Table 5 Measurement values obtained compared to IEEE 519-2014

Calculation of Total Demand Distortion (TDD)

Total Demand Distortion or TDD evaluates the harmonic currents that occur between the user and the power supply.

Harmonic values are based on a common point of coupling (PCC), which is a common point from which each user receives power from the power supply.

The power meter uses the following equation to calculate TDD,

$$TDD = \left(\frac{\sqrt{(HCIA)^2+(HCIB)^2+(HCIC)^2}}{(ILOAD)*100}\right)$$

Where ILoad equals the maximum demand load of the power system. Source: https://www.productinfo.schneider-electric.com/pm5300/5be97f3b347bdf0001d99c87/PM5300%20User%20Manual/Spanish/BM_PM5300UserManual_EAV15107_Spanish_Castilian_es_0000237456.ditamap/$/C_PQ_TDDCalculations_Spanish_Castilian_es_0000076995

Frequency profile

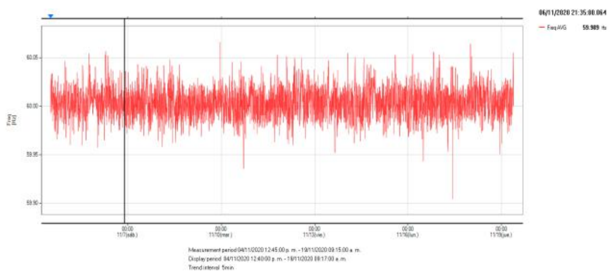

Figure 7 Maximum and minimum frequency profile

The graph shows the profile of the maximum and minimum frequency. The behavior of the average frequency is 60,004 Hz, minimum value 59,959 Hertz and its maximum value 60,049 Hertz. The average value is 0.006% above the value of the fundamental frequency of 60 Hertz. The variation window presents a maximum 0.08% above the value of the fundamental. The maximum values were presented instantaneously, however, these values do not affect the loads.

Measurements in the residential photovoltaic system

Voltage profile

In general, the 2 phases presented instantaneous variations (figure 8). The values were compared with the standard IEEE 1100-1999 variation not greater than 5% and with the regulation of the law of the electric power public service, chapter V article 18 variation not greater than 10%;

Phase 1 presents an average 6.6% above the nominal value (127 V), phase 2 presents an average 7.62% above the nominal value (127 V), the two phases can be classified as out of range under the IEEE 1100- standard 1999 but within the regulations of the law of the electric power public service.

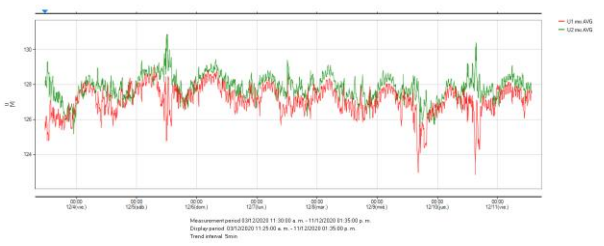

Figure 8 Graph of voltage profile in PV system of 2 kWp

Phase	Nominal phase-to-neutral voltage	Phase-to-neutral voltage (V) Minimum	Average	Maximum	Limits	IEEE Std 1100-1999
1	127 V	107.57	127.12	127.53	± 5%	No complies
2	127 V	127.22	127.83	128.43		Complies

Table 6 Voltage limits

Note: In phase 1 the minimum value marks 107.57 on December 4, 2020 at 1:50 p.m., this value was caused by a CFE failure.

Current profile

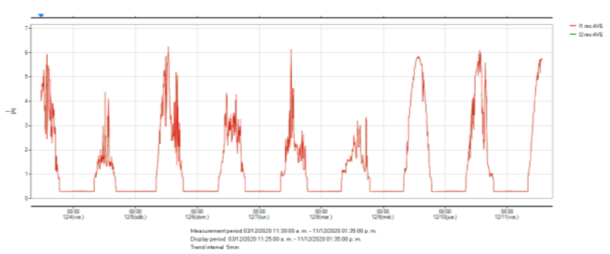

Figure 9 Graph of current profile in PV system of 2 kWp.

Graph 9 shows the behavior of the 2 phases, which present a balanced behavior, registering maximum values of 6.25 A per phase in the period of time between 12h00 and 13h00. The variation in amperage is not periodic and is caused by variations in solar irradiance in the solar panels. Throughout the monitoring period, there were no other disturbances that affect the quality of energy with reference to the current.

Power profile

In general, in graph 8, the 2 phases presented a maximum individual real power (kW) of 0.7 kW and a total of 1.5 kW. The values are reasonable considering that it has an installed photovoltaic capacity of 2 kWp.

Since it is not an efficiency study, the comparative alternating current power VS photovoltaic power is not made.

The lower part of the graph shows the behavior of the power factor throughout the measurement period. Due to the type of system in question, electricity generation from a linear signal can have a power factor of practically 1, in this case, its average value was oscillating throughout the operation time from 0.8 to 0.99. Most brands allow you to adjust the power factor by limiting other parameters. Measurements were made with original factory settings.

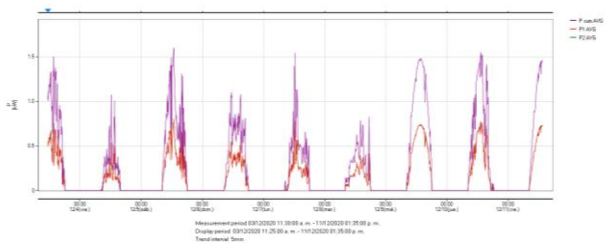

Figure 10 Graph of the power profile in PV system of 2 kWp

Phase	Nominal phase to neutral voltage	Phase-to-neutral voltage (V) Minimum	Average	Máximum	Límits	IEEE Std 1100-1999
1	127 V	107.57	127.12	127.53	± 5%	Fails
2	127 V	127.22	127.83	128.43		Complies

Table 7 Measured values obtained

Harmonic component profile of voltage and current

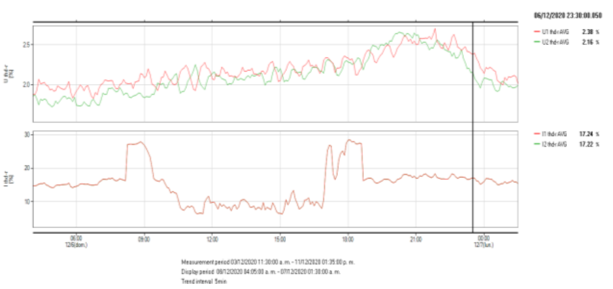

Figure 11 Profile graph of the harmonic component of voltage and current in PV system of 2 kWp.

Graph 11 shows the behavior of the inverter, with early morning being the left side and nighttime being the right side, the upper part of the graph shows the total harmonic distortion of voltage THDv and the lower part the total harmonic distortion in current THDi. In graph 8 you can see that during the operation of the inverter it shows average THDi values of 6.23% in each phase and a practically periodic voltage harmonic distortion behavior of 2.42% of THDv.

ISSN-2523-2517

This is due to the fact that all the time the inverter is receiving a potential difference at the measurement point and this will be the value of the grid, as opposed to the current. This only shows reading when the inverter is injecting energy into the grid and is capable of controlling the harmonic contribution, at night, as it does not have a generation and the equipment goes to "rest state", there is no current flow through what the reading you have may be due to interference or noise due to a zero value or milliamp readings. The manufacturer of the inverter in its data sheet shows a THDv of <3%, for the THDv the maximum value reached in the measurements is approximately 2.5%, comparing the values with table 1 of the IEEE Std 519-2014, it is observed that it complies with this index of total harmonic distortion in voltage.

Table 1—Voltage distortion limits

Bus voltage V at PCC	Individual harmonic (%)	Total harmonic distortion THD (%)
$V \leq 1.0$ kV	5.0	8.0
1 kV < $V \leq$ 69 kV	3.0	5.0
69 kV < $V \leq$ 161 kV	1.5	2.5
161 kV < V	1.0	1.5[a]

[a]High-voltage systems can have up to 2.0% THD where the cause is an HVDC terminal whose effects will have attenuated at points in the network where future users may be connected.

Source: https://edisciplinas.usp.br/pluginfile.php/1589263/mod_resource/content/1/IEE%20Std%20519-2014.pdf

Phase	THDV Máx.	Maximum limit (%)	Std. IEEE 519-2014
1	2.42	8%	Complies
2	1.93		Complies
3	N/A		N/A

Table 8 Measurement values obtained compared to IEEE 519-2014

Frequency profile

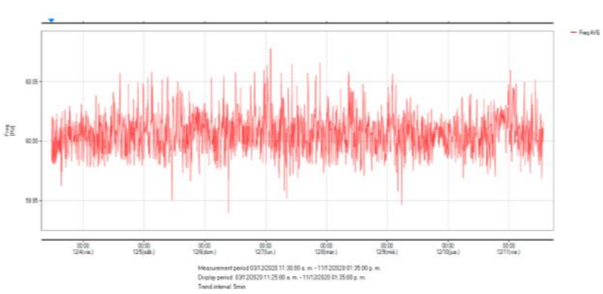

Figure 12 Frequency profile

The graph shows the profile of the maximum and minimum frequency. The behavior of the average frequency is 60,078 Hz, minimum value 60,039 Hertz and its maximum value 60,273 Hertz. The average value is 0.12% above the value of the fundamental frequency of 60 Hertz.

The variation window presents a maximum 0.45% above the value of the fundamental. The maximum values were presented instantaneously, however, these values do not affect the loads.

Discussion

According to the data recorded in the commercial photovoltaic system using a Fronius® inverter of Austrian origin, acceptable values were found in voltage, current, power, PF and harmonics. Although it has a harmonic distortion, it is low and the individual contribution it can make is 0.05 Amp. Harmonic orders do not represent a possibility of damage to specific loads connected to the network. Graph 12 shows the behavior of the voltage waveform, the THDV is 1.52%. No other disturbances affecting power quality are observed during the measurement period.

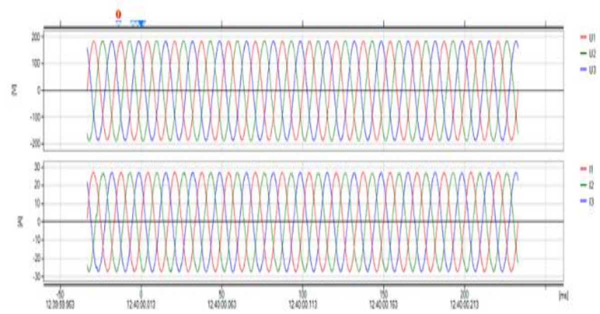

Figure 14 Waveform of a commercial photovoltaic system

On the other hand, the residential photovoltaic system uses a GOODWE® inverter made in Shanghai meets off-grid values, but these are not attributable to the inverter, but to the grid. The current behavior is stable as is the power. Harmonics are integer multiples of the fundamental frequency, this disturbance that affects the quality of power, the presence of harmonics in residential, commercial and industrial electrical systems, causes heating of conductors, tripping of protections and the effects are maximized when the voltage occurs. series or parallel resonance which contributes to the damage of sensitive electronic equipment. It is necessary to know the response of the industrial electrical system, which can be known by performing a frequency sweep to know the frequency at which the series or parallel resonance could occur.

The individual contribution continues to be low, during the measurement period harmonics of 3rd order (3.05%), 5th order (1.82%), 7th order (1.7%) and with a higher contribution of 9th order (4.25%) were identified. Figure 10 shows the waveform of the residential inverter, a distorted wave can be seen on the crest and this distortion is caused by the afore mentioned harmonics.

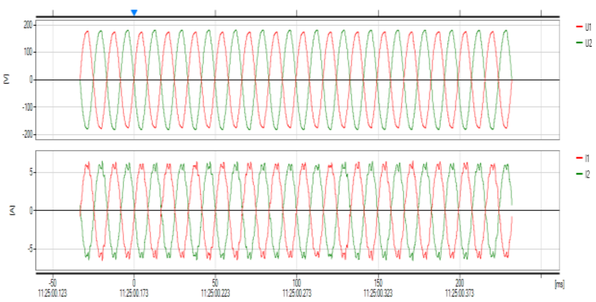

Figure 13 Waveform of a domestic photovoltaic system

Conclusions

The degree to which harmonics can be tolerated is determined by the susceptibility of the load (or power source) to them. The least susceptible type of equipment is one in which the main function is in heating, such as in an oven. In this case, harmonic energy is generally used and is therefore completely tolerable. The most susceptible type of equipment is that whose design or constitution assumes a (almost) perfect sinusoidal fundamental input.

This equipment is frequently found in the categories of communication or data processing equipment. One type of load that normally falls between these two extremes of susceptibility is motor load. Most motor loads are relatively tolerant of harmonics. Even for the least susceptible equipment, harmonics can be damaging. In the case of a furnace, for example, they can cause thermal dielectric stress or stress, which causes premature aging of the electrical insulation.

Broadly speaking, it can be concluded that a photovoltaic system can deliver a different quality of energy between inverter manufacturers and this could be directly related to the price. The better power quality you deliver, the more specific electronics you will need, increasing your cost.

Now, this power quality cannot be enough to say that it will cause failures in the grid or electrical appliances, these damages are associated with a combined situation between the inverter, the grid and electrical appliances, that is, resonance. These impact studies are recommended to be done in photovoltaic systems connected to industrial electrical installations.

In the two cases studied, we found effects greater than 5% established in the IEEE 1100-1999 standard, but less than 10% established in the Mexican legal framework, in accordance with CFE Specification L0000-45 "Permissible deviations in waveforms of voltage and current in the supply and consumption of electrical energy, which do not cause damage to the electronic cards of the equipment used in the Mexican hotel industry".

Acknowledgments

The authors are grateful for the facilities provided by the company "MATERIALES LA VENA", as well as the owner of the house to carry out the analysis within their PV system interconnected to the grid, they also thank the Technological University of Bahía de Banderas, Nayarit and Technological University of San Juan del Río, Querétaro for its willingness to do so loan of Hioki® power quality analyzer equipment.

References

Afonso, T., de Arruda Bitencourt, L., Fortes, M., Gomes, J., & Maciel, R. (2018). Impact Analysis on Power Quality of a Small Distributed Generation. *American Journal of Renewable and Sustainable Energy, 4*(3), 56-63.

Bouchakour, S., Chouder, A., Cherfa, F., Abdeladim, K., & Kerkouche, K. (2012). The First Grid-Connected Photovoltaic System in Algeria: Power Quality Observation. *The Second International Days on Renewable Energies & Sustainable Development*, (págs. 1-6). Argelia.

Caballero, C., Cortez, L., Muñoz, G., & Castañeda, J. (2016). Filtro activo de potencia para compensar la distorsión armónica de un sistema fotovoltaico autónomo. *Tecnología e Inovación, 3*(9), 76-84.

ISSN-2523-2517

Çelebi, A., & Çolak, M. (2011). The effects of harmonics produced by Grid connected photovoltaic systems on electrical networks. . *Universities Power Engineering Conference (UPEC) Proceedings of* , (págs. 1-8). Izmir.

Durán, J. C., Raggio, D., Socolovsky, H. P., Videla, M., & Plá, J. (2016). Evaluación de la calidad de la energía en dos casos de estudio: distorsión armónica inyectada por un sistema fotovoltaico de 40 kw y emitida por las cargas de una vivienda unifamiliar. . *Avances en Energías Renovables y Medio Ambiente-AVERMA*(20), 1-12.

Favuzza, S., Graditi, G., Spertino, F., & Vitale, G. (2004). Comparison of power quality impact of different photovoltaic inverters: the viewpoint of the grid. *IEEE International Conference on Industrial Technology, 2004.*, (págs. 542-547).

Gallo, D., Landi, C., Luiso, M., & Edoardo, F. (2013). Analysis of a photovoltaic system: AC and DC power quality. *WSEAS Transactions on Power Systems, 8*(4), 45-55.

González, P., Romero-Cadaval, E., G. E., & Guerrero, M. A. (2011). Impact of grid connected photovoltaic system in the power quality of a distribution network. (págs. 466-473). Springer.

González-Castrillo, P., Romero-Cadaval, E., González-Romera, E., Barrero-González, F., & Guerrero-Martínez, M. A. (2007). Influencia de una Instalación Fotovoltaica Conectada a Red sobre la Calidad de Potencia de una Red de Distribución. Extremadura, España.

Hernández, J. C., & Medina, A. (2006). Conexión de sistemas fotovoltaicos a la red eléctrica: calidad de suministro. *Sumuntán*(23), 33-44.

Lu, S. Y., Wang, L., Ke, S. C., Chang, C. H., & Yang, Z. H. (2014). Analysis of measured power-quality results of a PV system connected to Peng-Hu Power System. *IEEE Industry Application Society Annual Meeting* , (págs. 1-7).

Misak, S., Prokop, L., & Bilik, P. (2014). Power quality analysis in off-grid power system. *ELEKTRO*, 337-342.

Niitsoo, J., Jarkovoi, M., Taklaja, P., Klüss, J., & Palu, I. (2015). Power quality issues concerning photovoltaic generation in distribution grids. *Smart Grid and Renewable Energy*, 1-6.

Patsalides, M., Evagorou, D., Makrides, G., Achillides, Z., Georghiou, G. E., Stavrou, A., & Werner, J. H. (2007). The effect of solar irradiance on the power quality behaviour of grid connected photovoltaic systems. *RE&PQJ*, 1-7.

Ruelas, R. (12-26 de abril de 2021). Sistemas de Puesta a Tierra [Curso de Capacitación]. . Querétaro, Querétaro, México: Instituto de Ingenieros en Electricidad y Electrónica IEEE PES Querétaro-Guanajuato.

SEMARNAT. (2020). *Guía de eficiencia energética en el diseño, construcción y operación de hoteles en climas cálidos.* Obtenido de https://www.gob.mx/semarnat/documentos/guia-de-eficiencia-energetica-en-el-diseno-construccion-y-operacion-de-hoteles-en-climas-calidos

Spertino, F., Chicco, G., Ciocia, A., Malgaroli, G., Mazza, A., & Russo, A. (2018). Harmonic distortion and unbalance analysis in multi-inverter photovoltaic systems. *2018 International Symposium on Power Electronics, Electrical Drives, Automation and Motion (SPEEDAM)* (págs. 1031-1036). IEEE.

[[Title in Times New Roman and Bold No. 14 in English and Spanish]

Surname (IN UPPERCASE), Name 1st Author†*, Surname (IN UPPERCASE), Name 1st Coauthor, Surname (IN UPPERCASE), Name 2nd Coauthor and Surname (IN UPPERCASE), Name 3rd Coauthor

Institutional Affiliation of Author including Dependency (No.10 Times New Roman and Italic)

International Identification of Science - Technology and Innovation

ID 1st Author: (ORC ID - Researcher ID Thomson, arXiv Author ID - PubMed Author ID - Open ID) and CVU 1st author: (Scholar-PNPC or SNI-CONACYT) (No.10 Times New Roman)

ID 1st Coauthor: (ORC ID - Researcher ID Thomson, arXiv Author ID - PubMed Author ID - Open ID) and CVU 1st coauthor: (Scholar or SNI) (No.10 Times New Roman)

ID 2nd Coauthor: (ORC ID - Researcher ID Thomson, arXiv Author ID - PubMed Author ID - Open ID) and CVU 2nd coauthor: (Scholar or SNI) (No.10 Times New Roman)

ID 3rd Coauthor: (ORC ID - Researcher ID Thomson, arXiv Author ID - PubMed Author ID - Open ID) and CVU 3rd coauthor: (Scholar or SNI) (No.10 Times New Roman)

(Report Submission Date: Month, Day, and Year); Accepted (Insert date of Acceptance: Use Only ECORFAN)

Abstract (In English, 150-200 words)

Objectives
Methodology
Contribution

Keywords (In English)

Indicate 3 keywords in Times New Roman and Bold No. 10

Abstract (In Spanish, 150-200 words)

Objectives
Methodology
Contribution

Keywords (In Spanish)

Indicate 3 keywords in Times New Roman and Bold No. 10

Citation: Surname (IN UPPERCASE), Name 1st Author, Surname (IN UPPERCASE), Name 1st Coauthor, Surname (IN UPPERCASE), Name 2nd Coauthor and Surname (IN UPPERCASE), Name 3rd Coauthor. Paper Title. Journal Electrical Engineering. Year 1-1: 1-11 [Times New Roman No.10]

* Correspondence to Author (example@example.org)
† Researcher contributing as first author.

Month, Year Vol.1 No.1 1-15-[Using ECORFAN]

Introduction

Text in Times New Roman No.12, single space.

General explanation of the subject and explain why it is important.

What is your added value with respect to other techniques?

Clearly focus each of its features

Clearly explain the problem to be solved and the central hypothesis.

Explanation of sections Article.

Development of headings and subheadings of the article with subsequent numbers

[Title No.12 in Times New Roman, single spaced and bold]

Products in development No.12 Times New Roman, single spaced.

Including graphs, figures and tables-Editable

In the article content any graphic, table and figure should be editable formats that can change size, type and number of letter, for the purposes of edition, these must be high quality, not pixelated and should be noticeable even reducing image scale.

[Indicating the title at the bottom with No.10 and Times New Roman Bold]

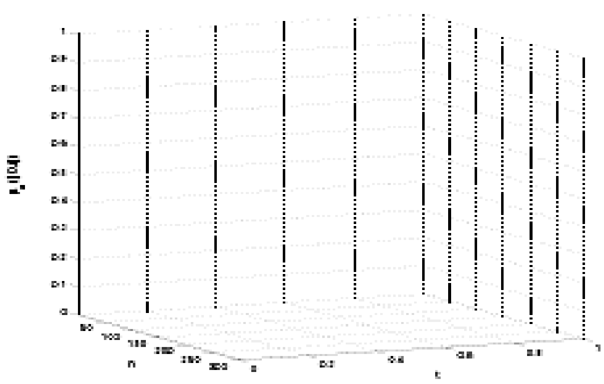

Graphic 1 Title and *Source (in italics)*

Should not be images-everything must be editable.

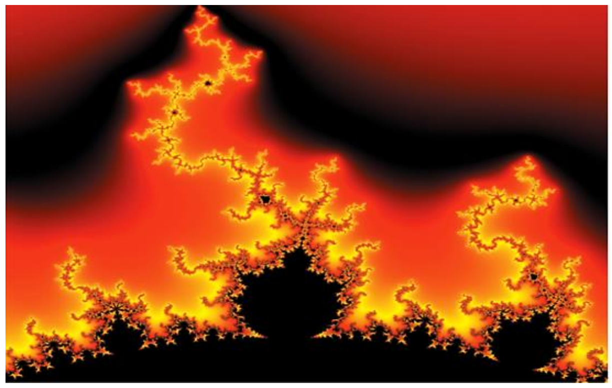

Figure 1 Title and *Source (in italics)*

Should not be images-everything must be editable.

Table 1 Title and *Source (in italics)*

Should not be images-everything must be editable.

Each article shall present separately in **3 folders**: a) Figures, b) Charts and c) Tables in .JPG format, indicating the number and sequential Bold Title.

For the use of equations, noted as follows:

$$Y_{ij} = \alpha + \sum_{h=1}^{r} \beta_h X_{hij} + u_j + e_{ij} \qquad (1)$$

Must be editable and number aligned on the right side.

Methodology

Develop give the meaning of the variables in linear writing and important is the comparison of the used criteria.

Results

The results shall be by section of the article.

Annexes

Tables and adequate sources

Thanks

Indicate if they were financed by any institution, University or company.

ISSN 2523-2517

Conclusions

Explain clearly the results and possibilities of improvement.

References

Use APA system. Should not be numbered, nor with bullets, however if necessary numbering will be because reference or mention is made somewhere in the Article.

Use Roman Alphabet, all references you have used must be in the Roman Alphabet, even if you have quoted an Article, book in any of the official languages of the United Nations (English, French, German, Chinese, Russian, Portuguese, Italian, Spanish, Arabic), you must write the reference in Roman script and not in any of the official languages.

Technical Specifications

Each article must submit your dates into a Word document (.docx):

Journal Name
Article title
Abstract
Keywords
Article sections, for example:

1. Introduction
2. Description of the method
3. Analysis from the regression demand curve
4. Results
5. Thanks
6. Conclusions
7. References

Author Name (s)
Email Correspondence to Author
References

Intellectual Property Requirements for editing:

-Authentic Signature in Color of Originality Format Author and Co-authors.

-Authentic Signature in Color of the Acceptance Format of Author and Co-authors.

Reservation to Editorial Policy

Journal Electrical Engineering reserves the right to make editorial changes required to adapt the Articles to the Editorial Policy of the Research Journal. Once the Article is accepted in its final version, the Research Journal will send the author the proofs for review. ECORFAN® will only accept the correction of errata and errors or omissions arising from the editing process of the Research Journal, reserving in full the copyrights and content dissemination. No deletions, substitutions or additions that alter the formation of the Article will be accepted.

Code of Ethics - Good Practices and Declaration of Solution to Editorial Conflicts

Declaration of Originality and unpublished character of the Article, of Authors, on the obtaining of data and interpretation of results, Acknowledgments, Conflict of interests, Assignment of rights and Distribution

The ECORFAN-Mexico, S.C. Management claims to Authors of Articles that its content must be original, unpublished and of Scientific, Technological and Innovation content to be submitted for evaluation.

The Authors signing the Article must be the same that have contributed to its conception, realization and development, as well as obtaining the data, interpreting the results, drafting and reviewing it. The Corresponding Author of the proposed Article will request the form that follows.

Article title:

– The sending of an Article to Journal Electrical Engineering emanates the commitment of the author not to submit it simultaneously to the consideration of other series publications for it must complement the Format of Originality for its Article, unless it is rejected by the Arbitration Committee, it may be withdrawn.

– None of the data presented in this article has been plagiarized or invented. The original data are clearly distinguished from those already published. And it is known of the test in PLAGSCAN if a level of plagiarism is detected Positive will not proceed to arbitrate.

– References are cited on which the information contained in the Article is based, as well as theories and data from other previously published Articles.

– The authors sign the Format of Authorization for their Article to be disseminated by means that ECORFAN-Mexico, S.C. In its Holding Republic of Peru considers pertinent for disclosure and diffusion of its Article its Rights of Work.

– Consent has been obtained from those who have contributed unpublished data obtained through verbal or written communication, and such communication and Authorship are adequately identified.

– The Author and Co-Authors who sign this work have participated in its planning, design and execution, as well as in the interpretation of the results. They also critically reviewed the paper, approved its final version and agreed with its publication.

– No signature responsible for the work has been omitted and the criteria of Scientific Authorization are satisfied.

– The results of this Article have been interpreted objectively. Any results contrary to the point of view of those who sign are exposed and discussed in the Article.

Copyright and Access

The publication of this Article supposes the transfer of the copyright to ECORFAN-Mexico, SC in its Holding Republic of Peru for its Journal Electrical Engineering, which reserves the right to distribute on the Web the published version of the Article and the making available of the Article in This format supposes for its Authors the fulfilment of what is established in the Law of Science and Technology of the United Mexican States, regarding the obligation to allow access to the results of Scientific Research.

Article Title:

Name and Surnames of the Contact Author and the Co-authors	Signature
1.	
2.	
3.	
4.	

Principles of Ethics and Declaration of Solution to Editorial Conflicts

Editor Responsibilities

The Publisher undertakes to guarantee the confidentiality of the evaluation process, it may not disclose to the Arbitrators the identity of the Authors, nor may it reveal the identity of the Arbitrators at any time.

The Editor assumes the responsibility to properly inform the Author of the stage of the editorial process in which the text is sent, as well as the resolutions of Double-Blind Review.

The Editor should evaluate manuscripts and their intellectual content without distinction of race, gender, sexual orientation, religious beliefs, ethnicity, nationality, or the political philosophy of the Authors.

The Editor and his editing team of ECORFAN® Holdings will not disclose any information about Articles submitted to anyone other than the corresponding Author.

The Editor should make fair and impartial decisions and ensure a fair Double-Blind Review.

Responsibilities of the Editorial Board

The description of the peer review processes is made known by the Editorial Board in order that the Authors know what the evaluation criteria are and will always be willing to justify any controversy in the evaluation process. In case of Plagiarism Detection to the Article the Committee notifies the Authors for Violation to the Right of Scientific, Technological and Innovation Authorization.

Responsibilities of the Arbitration Committee

The Arbitrators undertake to notify about any unethical conduct by the Authors and to indicate all the information that may be reason to reject the publication of the Articles. In addition, they must undertake to keep confidential information related to the Articles they evaluate.

Any manuscript received for your arbitration must be treated as confidential, should not be displayed or discussed with other experts, except with the permission of the Editor.

The Arbitrators must be conducted objectively, any personal criticism of the Author is inappropriate.

The Arbitrators must express their points of view with clarity and with valid arguments that contribute to the Scientific, Technological and Innovation of the Author.

The Arbitrators should not evaluate manuscripts in which they have conflicts of interest and have been notified to the Editor before submitting the Article for Double-Blind Review.

Responsibilities of the Authors

Authors must guarantee that their articles are the product of their original work and that the data has been obtained ethically.

Authors must ensure that they have not been previously published or that they are not considered in another serial publication.

Authors must strictly follow the rules for the publication of Defined Articles by the Editorial Board.

The authors have requested that the text in all its forms be an unethical editorial behavior and is unacceptable, consequently, any manuscript that incurs in plagiarism is eliminated and not considered for publication.

Authors should cite publications that have been influential in the nature of the Article submitted to arbitration.

Information services

Indexation - Bases and Repositories

RESEARCH GATE (Germany)
GOOGLE SCHOLAR (Citation indices-Google)
MENDELEY (Bibliographic References Manager)
HISPANA (Information and Bibliographic Orientation-Spain)

Publishing Services

Citation and Index Identification H
Management of Originality Format and Authorization
Testing Article with PLAGSCAN
Article Evaluation
Certificate of Double-Blind Review
Article Edition
Web layout
Indexing and Repository
ArticleTranslation
Article Publication
Certificate of Article
Service Billing

Editorial Policy and Management

1047 La Raza Avenue -Santa Ana, Cusco-Peru. Phones: +52 1 55 6159 2296, +52 1 55 1260 0355, +52 1 55 6034 9181; Email: contact@ecorfan.org www.ecorfan.org

ECORFAN®

Chief Editor
QUINTANILLA - CÓNDOR, Cerapio. PhD

Executive Director
RAMOS-ESCAMILLA, María. PhD

Editorial Director
PERALTA-CASTRO, Enrique. MsC

Web Designer
ESCAMILLA-BOUCHAN, Imelda. PhD

Web Diagrammer
LUNA-SOTO, Vladimir. PhD

Editorial Assistant
TREJO-RAMOS, Iván. BsC

Translator
DÍAZ-OCAMPO, Javier. BsC

Philologist
RAMOS-ARANCIBIA, Alejandra. BsC

Advertising & Sponsorship

(ECORFAN® Republic of Peru), sponsorships@ecorfan.org

Site Licences

03-2010-032610094200-01-For printed material ,03-2010-031613323600-01-For Electronic material,03-2010-032610105200-01-For Photographic material,03-2010-032610115700-14-For the facts Compilation,04-2010-031613323600-01-For its Web page,19502-For the Iberoamerican and Caribbean Indexation,20-281 HB9-For its indexation in Latin-American in Social Sciences and Humanities,671-For its indexing in Electronic Scientific Journals Spanish and Latin-America,7045008-For its divulgation and edition in the Ministry of Education and Culture-Spain,25409-For its repository in the Biblioteca Universitaria-Madrid,16258-For its indexing in the Dialnet,20589-For its indexing in the edited Journals in the countries of Iberian-America and the Caribbean, 15048-For the international registration of Congress and Colloquiums. financingprograms@ecorfan.org

Management Offices

1047 La Raza Avenue -Santa Ana, Cusco-Peru.

Journal Electrical Engineering

"Analysis of objective functions and weighting parameters syntonization for protection optimization"
SHIH, Meng Yen, LEZAMA-ZÁRRAGA, Francisco Román, CHAN-GONZALEZ, Jorge de Jesús and SALAZAR-UTIZ, Ricardo Rubén
Universidad Autónoma de Campeche

"AC home appliances in a DC home nanogrid"
CORDOVA-FAJARDO, Miguel Ángel & TUTUTI, Eduardo S.
Instituto Tecnológico de Lázaro Cárdenas
Universidad Michoacana de San Nicolás de Hidalgo

"Prototype simulation for the measurement of energy consumption in watts for alternating current systems"
HERNÁNDEZ-LUNA, Aldo, CASTRO-JUÁREZ, Ana Magdalena, TORRES-JIMÉNEZ, Jacinto and HERNÁNDEZ-CABRERA, Hugo
Instituto Tecnológico Superior de Huauchinango

"Analysis of power quality in photovoltaic systems interconnected to the grid"
DIBENE-ARRIOLA, Luis Martin, FLETES-CAMACHO, Noé Guadalupe, PAREDES-VAZQUEZ, César Paul and MARROQUÍN-DE JESÚS, Ángel
Universidad Tecnológica de Bahía de Banderas
Universidad Tecnológica de San Juan del Río

ISSN 2523-2517
www.ecorfan.org